



**TRIBHUVAN UNIVERSITY
INSTITUTE OF ENGINEERING
PULCHOWK CAMPUS**

THESIS NO. PUL079MSGtE013

Numerical Analysis of Laterally Loaded Pile in Sandy Soil

by

Pooja Singh

A THESIS

SUBMITTED TO THE DEPARTMENT OF CIVIL ENGINEERING
IN PARTIAL FULFILLMENT OF THE REQUIREMENTS FOR THE
DEGREE OF
MASTER OF SCIENCE IN GEOTECHNICAL ENGINEERING

DEPARTMENT OF CIVIL ENGINEERING
LALITPUR, NEPAL

April, 2026

COPYRIGHT

The author has granted permission for this thesis to be made available for public reference by the library, the Department of Civil Engineering at Pulchowk Campus, and the Institute of Engineering. In addition, approval for substantial reproduction of this work for academic purposes may be provided by the supervising professor(s), or in their absence, by the Head of the Department where the research was conducted. Proper acknowledgment must be given to the author, the Department of Civil Engineering at Pulchowk Campus, and the Institute of Engineering whenever the material is used. Any reproduction, publication, or use of this thesis for commercial purposes is strictly prohibited without prior written consent from both the author and the Department of Civil Engineering, Pulchowk Campus, Institute of Engineering. Requests for permission to reproduce or use any part of this thesis, either in full or in part, should be directed to:

.....

Head of the Department
Department of Civil Engineering,
Pulchowk Campus, Institute of Engineering,
Pulchowk, Lalitpur, Nepal

TRIBHUVAN UNIVERSITY
INSTITUTE OF ENGINEERING
PULCHOWK CAMPUS
DEPARTMENT OF CIVIL ENGINEERING
PULCHOWK, LALITPUR

The thesis entitled “Numerical Analysis of Laterally Loaded Pile in Sandy Soil,” submitted by Mrs. Pooja Singh in partial fulfillment of the requirements for the Master of Science (M.Sc.) degree in Geotechnical Engineering, has been reviewed and approved for the award of the degree by Tribhuvan University.

The undersigned confirm that they have examined the thesis and recommend its acceptance by the Institute of Engineering as meeting the requirements for the Master of Science degree in Geotechnical Engineering.

.....
Supervisor
Asst. Prof. Dr. Bhim Kumar Dahal
Department of Civil Engineering
Institute of Engineering, Pulchowk Campus

.....
External Examiner
Er. Tuk Lal Adhikari
ITECO Nepal Pvt. Ltd

.....
Program Coordinator
Asst. Prof. Dr. Bhim Kumar Dahal
Department of Civil Engineering
Institute of Engineering, Pulchowk Campus

April, 2026

DECLARATION

I hereby affirm that the study entitled “Numerical Analysis of Laterally Loaded Pile in Sandy Soil” represents my own original research. All relevant contributions from other researchers have been properly acknowledged. I take full responsibility for the accuracy, validity, and integrity of the data and information presented in this work.

.....

Pooja Singh

079/MSGtE/013

MSc in Geotechnical Engineering

Date: 26th April, 2026

ACKNOWLEDGEMENT

I wish to express my deepest and sincere appreciation to my supervisor, Dr. Bhim Kumar Dahal, for giving me a unique opportunity to work on such an important topic. His continuous guidance, encouragement, and critical suggestions throughout the course of this study are greatly acknowledged. I consider myself fortunate to work under his supervision.

I would like to acknowledge all the faculty members of the Department of Civil Engineering for the knowledge and concepts they gave me during my studies at IOE, Pulchowk Campus.

I am equally thankful to my friends in the MSGtE/079 batch for their cooperation and intellectual suggestions. My sincere thanks also go to all those who gave valuable support, critical comments, suggestions, and advice on different stages of my research work.

Last but not least, I would like to start off by thanking my parents for their persuasion and continuous support throughout my academic perseverance. They were always there, cheering me up and standing by me through good and bad times, which motivated me to overcome the difficulties and led to this stage of my thesis.

Pooja Singh

079/MSGtE/013

26th April, 2026

ABSTRACT

Pile foundations are elongated structural components, typically fabricated from steel or reinforced concrete, that transmit loads to deeper, more stable strata of earth. They are extensively utilized in supporting infrastructures, including edifices, bridges, railway systems, hydropower facilities, dams, and slope stabilization projects. Bored piles are commonly utilized for bridge foundations in Nepal. This research examines the lateral load capability of piles with Plaxis-3D software. It also investigates the distribution of loads among a collection of laterally loaded piles and assesses the impact of p-multipliers on their performance.

The settlement data obtained from routine pile load tests for bored piles of one of the test piles of the Mahuli Khola Bridge in Saptari district has been utilized. The Mohr-Coulomb constitutive model is employed in Plaxis-3D analysis, utilizing soil modeling data from the borehole log of Mahuli Khola, with additional parameters from the field and laboratory investigation. The model is validated by the curve obtained from pile load test data and Plaxis-3D results for different values of modulus of elasticity and different interface interaction factors. After the model validation, the same model is used for lateral load analysis, where a deflection limit of 1% of the diameter is considered, and the results are further verified through analysis by the L-Pile software.

Lateral load analysis is conducted for grouped pile configurations with varying quantities of piles arranged in distinct patterns. The lateral force carried by each row pile is evaluated for pile arrangements of (2×2 to 10×10) for spacing 3D, 5D, and 7D, and the p-multiplier effect for each row pile is determined by utilizing the lateral force for both single pile and group piles.

Keywords: Lateral load capacity, Mohr-Coulomb constitutive model, Numerical analysis, p-multiplier effect.

TABLE OF CONTENTS

COPYRIGHT.....	i
DECLARATION.....	iii
ACKNOWLEDGEMENT.....	iv
ABSTRACT.....	v
TABLE OF CONTENTS.....	vi
LIST OF FIGURES.....	ix
LIST OF TABLES.....	xi
ABBREVIATION AND SYMBOLS.....	xii
1 Introduction.....	1
1.1 Background.....	1
1.1 Problem Statement and Research Gaps.....	2
1.2 The objective of the Study.....	5
1.3 Scope.....	5
1.4 Limitations.....	5
2 Literature Review.....	6
2.1 Introduction to Piles.....	6
2.2 Laterally Loaded Pile.....	6
2.3 Soil-Pile Interaction in Sand.....	7
2.4 Lateral Load- Displacement Relationship.....	8
2.5 Pile Group Behavior Under Lateral Loading.....	8
2.6 Concept of p-multiplier.....	9
2.7 Load Test on Pile.....	10
2.8 Finite Element Method.....	12
2.9 Site Description.....	13
2.9.1 Geology of the site.....	14
2.9.2 Geo-mechanical Parameters.....	14
3 RESEARCH METHODOLOGY.....	17
3.1 Geometry.....	18
3.1.1 Meshing.....	19

3.1.2	Boundary condition.....	21
3.1.3	Pile as volume beam element.....	23
3.2	Geo-mechanical Parameters.....	24
3.2.1	Data collection	24
3.2.2	Soil exploration and properties	24
3.2.3	Sub-soil properties	24
3.2.4	Mohr-Coulomb parameters.....	25
3.3	Pile and Pile Properties	27
3.4	Routine Pile Load Test.....	28
3.5	Lateral Load Analysis on Single Pile and Group Pile.....	29
3.6	Finite Element Method.....	30
3.7	Numerical Analysis	30
3.8	L-pile Software.....	31
4	RESULTS AND DISCUSSION.....	32
4.1	Model Validation of Plaxis-3D Model Using Field Load Test Data	32
4.2	Lateral Load Response of a Single Pile Using Plaxis-3D.....	35
4.2.1	Effect of meshing on the model.....	35
4.2.2	Effect of the interface interaction factors R_{inter}	36
4.2.3	Effect of diameter	36
4.2.4	Effect of pile length	37
4.2.5	Effect of water level variations	38
4.2.6	Verification of Plaxis-3D results with L-Pile	39
4.3	Lateral Load Behaviour of Group Pile Analysis.....	40
4.3.1	Effect of pile spacing	40
4.3.2	Load-sharing behavior of piles in groups	41
4.3.3	Effect of pile spacing on shear force distribution	41
4.3.4	Evaluation of p-multiplier for group pile.....	50
4.3.5	Effect of pile spacing on p-multiplier	58
5	CONCLUSIONS AND RECOMMENDATIONS	60

5.1	Conclusions	60
5.2	Recommendations	61
6	REFERENCES	62
7	ANNEXES	68
	Annex-I Paper Publication.....	68
	Annex-II Soil Exploration	74
	Annex-III Static Pile Load Test of Mahuli Bridge	75

LIST OF FIGURES

Figure 2.1: Concept of lateral load (S. Mukherjee & A. Dey, 2016).	7
Figure 2.2: p–y curves for single and pile groups (Brown et al., 1988).	9
Figure 2.3: Typical setup for pile load test in compression. (Sharma et al., 1984).	11
Figure 2.4: Typical setup for pile load test in compression (ASTM Institute, 1977).	12
Figure 2.5: Google map of site location.	14
Figure 2.6: Borehole log sheet.	16
Figure 3.1: Conceptual framework of the study.	18
Figure 3.2: Mesh model of Plaxis-3D for a single pile.	19
Figure 3.3: 3D soil elements (10-node tetrahedron) (Source: Plaxis).	21
Figure 3.4: FEM model after meshing.	21
Figure 3.5: Boundary conditions.	22
Figure 3.6: Pile as volume element.	23
Figure 3.7: Pile load test curve at the field.	29
Figure 4.1: Load vs settlement for $R_{inter}=0.5$.	33
Figure 4.2: Load vs settlement for $R_{inter}=0.67$.	33
Figure 4.3: Load vs settlement for $R_{inter}=0.8$.	34
Figure 4.4: Load vs settlement for $R_{inter}=1.0$.	34
Figure 4.5: Effect of meshing on displacement	36
Figure 4.6: Load vs displacement for interface interaction factor	36
Figure 4.7: Load vs displacement for varying diameter.	37
Figure 4.8: Load vs displacement for varying length and varying diameter.	38
Figure 4.9: Variation of displacement versus water table	39
Figure 4.10: Variation of lateral load capacity vs diameter for L-pile.	39
Figure 4.11: Pile group arrangement for 3×3 pile.	40
Figure 4.12: Variation of lateral displacement versus pile spacing.	41

Figure 4.13: Shear force single pile.	42
Figure 4.14: Variation of lateral force with row position for 2×4.	49
Figure 4.15: Variation of lateral force with row position for 3×4.	49
Figure 4.16: Variation of lateral force with row position for 4×4.	49
Figure 4.17: Variation of lateral force with row position for 5×4.	50
Figure 4.18: Variation of p-multiplier vs spacing (s/d) for pile arrangement 2×2.	58
Figure 4.19: Variation of p-multiplier vs spacing (s/d) for pile arrangement 3×3.	59

LIST OF TABLES

Table 3.1: Material Data Set of the Plaxis volume pile	24
Table 3.2: Properties of the surrounding soil in Plaxis-3D (Gupta & Dahal, 2023b)..	26
Table 3.3: Test pile properties	27
Table 3.4: Load-Settlement data of routine Pile Load Test	28
Table 4.1: Average shear force for each row pile in the group pile for spacing 3D....	43
Table 4.2: Average shear force for each row pile in the group pile for spacing 5D....	44
Table 4.3: Average shear force for each row pile in the group pile for spacing 7D....	46
Table 4.4: p-multiplier factor for each row pile in the group pile for 3D.....	52
Table 4.5: p-multiplier factor for each row pile in the group pile for 5D.....	53
Table 4.6: p-multiplier factor for each row pile in the group pile for 7D.....	55

ABBREVIATION AND SYMBOLS

2D	Two Dimensional
3D	Three Dimensional
CIS	Cast-in-situ
CPT	Cone Penetration Test
DOR	Department of Roads
FDM	Finite Difference Method
FEA	Finite Element Analysis
FEM	Finite Element Method
HS	Hardening Soil
HSM	Hardening Soil Model
IS	Indian Standard
IRC	Indian Road Congress
kN	Kilo Newton
LE	Linear Elastic
MC	Mohr-Coulomb
mm	Millimeter
PDE	Partial Differential Equation
SPT	Standard Penetration Test

1 INTRODUCTION

Pile load capacity is a key consideration in foundation design because it defines how much load a pile can safely carry when placed in various ground conditions. Soils are broadly grouped into cohesive soils (such as clay) and cohesionless soils (such as sand), and each type has different characteristics that affect how piles perform and transfer loads. Conducting pile load tests is essential for both design verification and performance assessment. Since soil properties strongly control pile response and bearing capacity, it is necessary to carefully study how piles behave in sandy soils to ensure structural safety and stability.

1.1 Background

The pile load capacity is one of the most important factors in geotechnical engineering, as it suggests the maximum load that can be safely supported by a pile embedded in different types of soil. Soil characteristics—such as soil type, cohesion, friction angle, elastic modulus, and subgrade reaction—play a major role in determining the load-bearing capacity of piles.

Deep foundations are generally subject to lateral and vertical loads on structures. Lateral loads due to wind, water currents, ground pressure, and seismic pressures can have a significant effect on the performance and stability of pile foundations. The behavior of a pile subjected to lateral loading is influenced by various elements, including soil type, pile rigidity, boundary conditions, and load size. Conventional analytical and empirical approaches, including those proposed by IS 2911 and Broms' theory, frequently simplify soil-pile interaction and may fail to adequately represent the nonlinear behavior of soil, which can lead to inaccurate predictions of pile performance under lateral loads. Numerical modeling has improved considerably, making FEA methods such as Plaxis-3D very effective in simulating realistic soil-structure interactions. Plaxis-3D allows modeling of complex geometries, layered soils, and non-linear material properties, providing a complete analysis of the bending moments, lateral deflection, and soil reactions along the pile length. This numerical analysis allows a more accurate prediction of the behavior of the pile under lateral loads.

The response of piles subjected to lateral loads is very complex owing to the nonlinear interaction between the pile and the adjacent soil. This complexity becomes further complicated in the case of pile groups, where the interaction among neighboring piles results in diminished lateral rigidity and capacity relative to isolated individual piles. Pile spacing, pile head fixity, soil type, and

loading condition all have significant effects on pile groups' lateral performance, making it difficult to predict their behavior using simple methodologies.

Piles enable the transfer of structural loads to deeper, more stable strata. You can install piles, which are elongated and slender columns, using driving, drilling, or cast-in-situ methods. Driven piles can be made of a variety of materials, such as concrete, steel, and wood. Piles are of concrete, cast-in-situ. Foundations serve as the supporting base for structures such as buildings, bridges, railway lines, power plants, and dams, and they are also relevant in areas prone to landslides. In regions where soil liquefaction may occur, pile foundations are commonly adopted to minimize settlement. These foundations are designed to withstand lateral loads, vertical loads, or a combination of both.

Numerical methods like FEM and FDM are employed to model the behavior of the pile under various loading conditions and to gain a better understanding of the interaction between the soil and the pile. These algorithms evaluate pile reactions according to soil conditions, geometry, load distribution, and boundary conditions. Through the assessment of pile carrying capacity, researchers and engineers may comprehend pile behavior under various conditions, thereby promoting the safety and reliability of deep foundation systems, improving construction techniques, and optimizing pile designs. This expertise can improve construction techniques and pile configurations.

In Nepal, the use of deep foundations—particularly pile foundations—is becoming increasingly common. Cast-in-situ bored piles are widely adopted for bridge construction where deep foundations are required. As a result, traditional well foundations are gradually being replaced by bored cast-in-situ piles, which now perform the role previously served by conventional well foundations.

Some of them are like Tila River Bridge (Siyala Kudari bazar, Jumla District), Mainawati River Bridge (Devipur, Siraha), Babai River Bridge (Tulsipur, Dang), Safa Khola Bridge (Brahampuri, Sarlahi), Kadiya Khola Bridge (Morang), etc. These bridges are successfully designed and approved by the concerned authorities.

1.1 Problem Statement and Research Gaps

Nepal is located in an active seismic belt of the Himalaya, where earthquakes induce large lateral forces on foundation systems (M. Laporte et al., 2021). Previous seismic occurrences in Nepal, notably the 2015 Gorkha Earthquake, have

illustrated that insufficient attention to lateral loading can result in significant pile head displacements, diminished serviceability, damage to superstructures, and, in severe instances, foundation failure (GEER Association, 2015; Hashash, 2015).

Pile foundations that support infrastructure, including bridges, offshore platforms, transmission towers, and marine buildings, can endure substantial lateral loads from wind, wave action, traffic forces, and seismic activity. The precise prediction of laterally loaded pile responses in sandy soil is crucial for secure and cost-effective foundation design (Marjanović et al., 2020).

The role of laterally loaded piles is governed by complex non-linear soil-pile interaction mechanisms, which depend on the soil density, pile geometry, embedment depth, and boundary conditions. Conventional analytical methods, such as the p-y curve approach, are commonly employed; however, these techniques oversimplify soil behavior and fail to adequately describe the three-dimensional nonlinear interactions between piles and adjacent sandy soil (Bouafia, 2023; L. C. Reese et al., 1974).

Field lateral load testing is a reliable source of information regarding the response of individual piles, but such testing is expensive and time-consuming, and limits its application in routine engineering practice. As a result, numerical modeling techniques have become increasingly important tools for predicting the behavior of laterally loaded piles under different loading and soil conditions (Zhang et al., 1999).

The response of pile groups to lateral loading markedly differs from that of individual piles due to interaction effects, including overlapping stress zones and shadowing effects among adjacent piles, which reduce lateral resistance and change bending behavior (Marjanović et al., 2020; M. C. McVay et al., 2000). Although many experimental and numerical investigations have explored how piles behave laterally in sandy soils, relatively few studies focus on validating numerical models using actual field test results. In addition, there is limited research that systematically examines both the behavior of single piles and the interaction effects within pile groups under consistent soil conditions.

Therefore, there is a need to develop a validated numerical model based on field test results and to perform a comprehensive parametric study to evaluate the behavior of single and grouped laterally loaded piles in sandy soil.

Despite the prevalent use of numerical modeling to forecast lateral pile behavior, numerous studies predominantly depend on laboratory-scale testing or theoretical assumptions instead of comprehensive field validation at full scale.

Field-based calibration is crucial for enhancing the accuracy of numerical predictions (Zhang et al., 1999).

Analytical approaches like the $p-y$ curve method provide simplified soil resistance models, but cannot fully capture the complex three-dimensional nonlinear soil-pile interactions observed in sandy soils (Marjanović et al., 2020; L. C. Reese et al., 1974).

Pile groups subjected to lateral loads behave differently from single piles, as the interaction between adjacent piles alters both the displacement pattern and the distribution of bending moments. The interaction effects continue to be challenging to forecast precisely using traditional design methodologies (M. C. McVay et al., 2000).

Most prior research examines either individual piles or groups of piles in isolation. A comprehensive computational framework that compares both systems under analogous sandy soil conditions remains rare and essential for enhancing the reliability of foundation design (Marjanović et al., 2020).

The present study differs from previously published numerical investigations conducted using Plaxis-3D in several important aspects. First, the numerical model developed in this research is validated using available field lateral load test data, which improves the reliability of simulation results compared to studies based only on theoretical assumptions or laboratory-scale experiments.

Second, this study performs a systematic parametric analysis of a single laterally loaded pile embedded in sandy soil by varying key parameters such as pile diameter, pile length, and soil properties under consistent modeling conditions.

Third, the study investigates the group interaction effect of laterally loaded piles in sandy soil and compares the response of pile groups with that of single piles within the same numerical framework. Such combined evaluation helps to better understand pile-soil-pile interaction behavior under lateral loading.

Therefore, the novelty of this research lies in the integration of field-validated numerical modeling with a comprehensive parametric study of both single pile and pile group behavior in sandy soil using a three-dimensional finite element approach.

1.2 The objective of the Study

The primary aim of this study is to conduct a numerical analysis of the lateral load capacity of piles in soil, in order to improve understanding of pile–soil interaction and pile performance under different conditions. The specific objectives are:

1. To prepare and validate Numerical modeling using field test data.
2. To perform a parametric analysis of the behavior of a single laterally loaded pile.
3. To analyze the group effect of a laterally loaded pile.

1.3 Scope

This thesis focuses on the lateral load resistance of pile foundations and pile groups in bridge substructures subjected to static loading conditions. The research aims to determine the critical depth affecting lateral resistance, examine soil-pile interaction factors, and evaluate the average lateral force carried by the pile in each row. Numerical modeling is utilized to evaluate the performance of individual piles and pile groups.

This study neglects cyclic loading effects, seismic loading circumstances, long-term settling behavior, construction-stage effects, and full-scale field testing. The analysis is confined to the specified soil conditions, pile dimensions, and parameters of the bridge case study within the project framework.

Note: Future work must address dynamic loading given Nepal’s seismicity.

1.4 Limitations

Limitations of this study include:

- The soil parameters can be varied for further study.
- Validation can be done by the lateral load analysis of the pile test.
- Other advanced models can be used and compared for better results.
- The lateral response observed in pile load tests can be analyzed and simulated using numerical methods.
- The simplified design methods and codes can be used to compare results.

2 LITERATURE REVIEW

2.1 Introduction to Piles

Piles are employed to transfer the pressure to the underlying bedrock or a more robust soil layer when one or more top soil strata are excessively compressible and insufficiently strong to bear the strain imposed by the superstructure (Vesic, 1977). Piles are fundamental components of deep foundations, providing stability and support for structures. They can be subjected to axial loads (vertical) and lateral loads (horizontal), each influencing their bearing capacity differently (Bowles & Guo, 1996). According to (Bowles & Guo, 1996) Piles are structural members of timber, concrete, and/or steel that are used to transmit surface loads to lower levels in the soil mass. Piles are widely used for several functions, including:

- To transfer structural loads through weak soil layers to deeper, stronger strata, carrying both vertical and lateral forces.
- To resist uplift and overturning forces, such as in basement structures below the groundwater level or towers subjected to wind loads.
- To densify loose, cohesionless soils through displacement and vibration during pile driving; such piles may be removed afterward if required.
- To reduce settlement where shallow foundations rest on weak or highly compressible soils.
- To improve soil stiffness beneath machine foundations, helping to control vibration amplitude and system frequency.
- To provide additional stability for bridge abutments and piers, especially in areas susceptible to scour.
- In offshore structures, to transfer loads from above the water surface through the water column into the seabed, where piles may be subjected to both vertical (including buckling) and lateral forces.

2.2 Laterally Loaded Pile

Lateral loads are critical for piles subjected to wind, seismic activity, or soil movement. Designing piles to resist lateral loads in sandy soils is a common challenge in foundation engineering (Brown et al., 1988). The lateral response of piled foundations is important in the design of structures that may be subjected to

lateral loads (Abdrabbo & Gaaver, 2012). Loads are in the order of 10–15% of the vertical loads in the case of onshore structures, while this value may exceed 30% in the case of offshore structures (S. Rao et al., 1998). The response of laterally loaded pile groups is a complicated soil–structure interaction problem (Abdrabbo & Gaaver, 2012). The ultimate lateral capacity of a pile is defined as the load at which the lateral deflection reaches 0.2 times the pile diameter on the load–deflection curve (Broms, 1964). A specified lateral deflection limit—such as 1% of the pile diameter in accordance with IRC:78-2014—is adopted as the allowable criterion. This displacement can arise from lateral loading, soil movement, or the effects of installation processes.

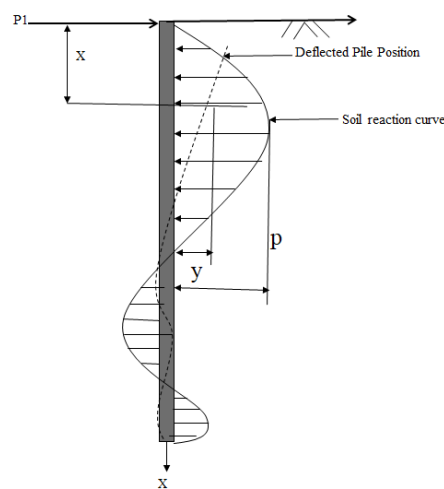


Figure 2.1: Concept of lateral load (S. Mukherjee & A. Dey, 2016).

2.3 Soil-Pile Interaction in Sand

The pile–soil interaction is a complex problem. Soil–structure interaction plays an important role in the behavior of structures under

static or dynamic loading (Kavitha et al., 2016). The behavior of laterally loaded piles is influenced by the relative stiffness of the pile with respect to the surrounding sand, which affects both the deformation pattern and the load-transfer mechanism along the pile shaft loading (Zhang et al., 2023). For pile groups in sandy soils, overlapping stress zones caused by the shadow effect reduce the effective soil resistance on adjacent piles and modify the p – y curves relative to those of individual piles (Zeng & Jiang, 2025). Experimental findings indicate that the response of piles to lateral loads in sandy soil is significantly affected by soil conditions at the surface and the pile tip, while the influence of intermediate soil layers is comparatively minimal (Lee et al., 2011). The lateral response of piles in

sandy soils is evaluated using the p–y curve method, in which the pile is treated as a beam and the surrounding soil is modeled as nonlinear springs that define the relationship between soil reaction (p) and lateral displacement (y) (Zhang et al., 1999). This method effectively captures nonlinear soil–structure interaction and has been extensively utilized in experimental and numerical studies of pile foundations (Kim & Jeong, 2011).

2.4 Lateral Load- Displacement Relationship

The lateral load–displacement behavior of piles in sand is nonlinear, depending on complex soil–pile interactions, and is essential for the predictive p–y curve models in the design and analysis of laterally loaded pile foundations (El Gendy, 2025). The Lateral load and displacement relationship presents that laterally applied horizontal load on a pile generates the lateral deflection at the pile head and along the shaft, which reflects the stiffness and soil resistance mobilized during loading (Poulos & Davis, 1980a) . From the study of (Lao et al., 2026), The load displacement curve shows that a relatively linear increase in lateral load with displacement is due to elastic soil response, which is followed by a nonlinear behavior as soil yielding and passive resistance mechanisms develop around the pile. Larger diameters and greater depths can increase lateral resistance (Poulos & Davis, 1980b). Finite element simulations of laterally loaded piles in sand reveal that the lateral load–displacement curves are strongly influenced by pile shape, loading direction, and pile length, with different pile geometries and loading orientations producing variations in the slope and curvature of the load–displacement response due to changes in mobilized soil support (Liu et al., 2025).

2.5 Pile Group Behavior Under Lateral Loading

Group piles respond differently than isolated piles because overlapping stress zones reduce lateral resistance, a phenomenon often termed the shadowing effect (McVay et al., 2000). (Brown et al., 1988)concluded that the pile group “was observed to deflect significantly more than the isolated single pile when loaded to a similar average load per pile. The “shadowing” effect was more considerable in sand compared to the clay, as was mentioned in (Brown et al., 1988). As pile spacing decreases, the interaction effects intensify, leading to a greater reduction in lateral resistance per pile and lower group efficiency, whereas increased spacing (greater than about 5–6 pile diameters) tends to diminish these interference effects and approach single-pile behaviour (Kavitha et al., 2016).

To account for the latter, the concept of a p-multiplier was developed (Brown et al., 1988).

2.6 Concept of p-multiplier

Lateral load tests on the group piles indicated distinct behavior from a single pile. The amount of lateral load carried by each pile in the group depends on its position (Zhou & Tokimatsu, 2018). This phenomenon is commonly known as the pile group effect. To account for the reduction in soil resistance during design, (Brown et al., 1988) introduced the concept of a p-multiplier. This factor is used to modify the lateral soil spring of a single pile to represent the behavior of piles within a group (Brown et al., 1988). Typically, the p-multiplier is assumed to remain constant for piles located within the same row.

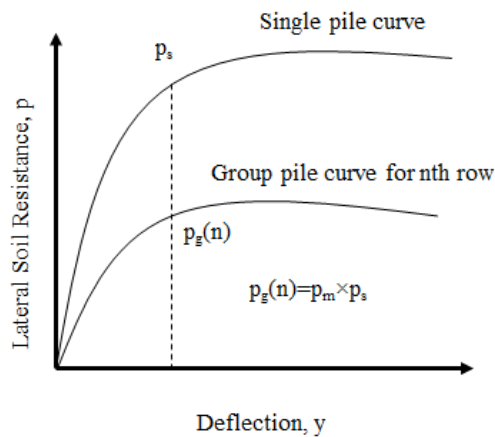


Figure 2.2: p - y curves for single and pile groups (Brown et al., 1988).

The p-multiplier can be obtained from the p - y curve as the ratio of the single pile soil resistance to that of the pile group. The p-multiplier (P_m) values of the leading piles were always greater than those obtained for the first and second trailing piles. The p- multipliers are 0.8, 0.4, and 0.3 for the leading pile, middle pile, and trailing pile. These values were obtained by judgment from values recommended by (M. McVay et al., 1998), (Chandrasekaran et al., 2010), (Rollins et al., 1998), (Brown et al., 1988), (Ilyas et al., 2004), (C. Reese et al., 2006), (Duncan & Wright, 2005), (FHWA, 1996). The available data cover piles installed in a variety of soil conditions. Previous studies show that the p-multiplier for leading-row piles typically ranges from 0.60 to 0.93, with an average of about 0.79. For second-row piles, values generally fall between 0.40 and 0.78, averaging around 0.58. In the third row, the range is approximately 0.40 to 0.63, with a mean near 0.46, while fourth-row piles exhibit values between 0.40 and 0.68, averaging about 0.52. However, adopting average values can be challenging due to variations in site conditions and interpretation methods. Moreover, the p-

multiplier is influenced by factors such as pile length and the relative stiffness of the pile–soil system. (Abdrabbo & Gaaver, 2012).

2.7 Load Test on Pile

The ultimate geotechnical capacity of a pile is commonly determined through a direct approach known as a pile load test. This method provides a relatively fast and dependable way to evaluate the load-bearing capacity of a pile in relation to the surrounding soil. Static load tests, in particular, are used to assess the pile's response—mainly under vertical loading—and are considered the most accurate for estimating both capacity and settlement behavior (IS 2911 (Part 4), 1985). As an in-situ technique, it is generally more reliable than indirect methods such as static or dynamic formulas and penetration test correlations, although it can be time-consuming to set up and carry out. Since there are so many variables to consider, it is especially difficult to establish a valid standard for determining the ultimate and safe bearing capacity of piles and predicting the behavior of pile groups from test data obtained from individual load tests on single piles (Shiva Saran Timalisina A, 2022). (IS 2911 (Part 4), 1985) is a code that provides a guideline to follow the standard procedure that is typically used in Nepal for load tests on piles. (IS 2911 (Part 4), 1985) specifies two types of tests, namely initial and routine tests for each type of loading (viz. vertical, lateral, and pullout).

Initial Test: Initial pile load tests are conducted for large or critical projects to confirm design assumptions. The number of tests may vary depending on the total number of piles and project requirements.

Routine Test: Routine testing is generally carried out on about 5% of the total piles. However, this percentage may be increased by up to an additional 2% based on the soil conditions and project specifications.

Vertical Load Test (Compression): A vertical compression test is performed to evaluate the axial load capacity and settlement characteristics of a pile under downward loading. In this procedure, a hydraulic jack applies load increments at the pile head, while settlement is carefully monitored at each stage. The test mobilizes both shaft friction and end-bearing resistance, enabling assessment of whether the pile can sustain the design load within acceptable settlement limits. These tests are commonly conducted using either the maintained load method (MLT) or the constant rate of penetration (CRP) method in accordance with standard guidelines, providing reliable in-situ data for design verification.

Maintained Load Method (MLT): This method is applicable for both initial and routine testing. Load is applied in increments, and displacement is recorded at each stage until the rate of movement at the pile head reduces to specified limits (e.g., 0.1 mm in 30 minutes, 0.2 mm in 1 hour, or within 2 hours, whichever occurs first). Each load stage is typically maintained for an extended period, often up to 24 hours.

Cyclic Method: The cyclic loading approach is mainly used during preliminary testing to separate shaft resistance from end-bearing resistance, particularly for piles with uniform cross-sections.

Constant Rate of Penetration (CRP) Method: This method is generally used for initial testing and involves applying load continuously at a constant penetration rate. Its load–settlement behavior differs from the maintained load method and is considered efficient for determining ultimate bearing capacity. However, it does not provide reliable information on settlement under working loads and is therefore not commonly used for routine testing.

Compression load tests were conducted using anchor piles, consistent with the procedure described by Sharma et al. (1984).

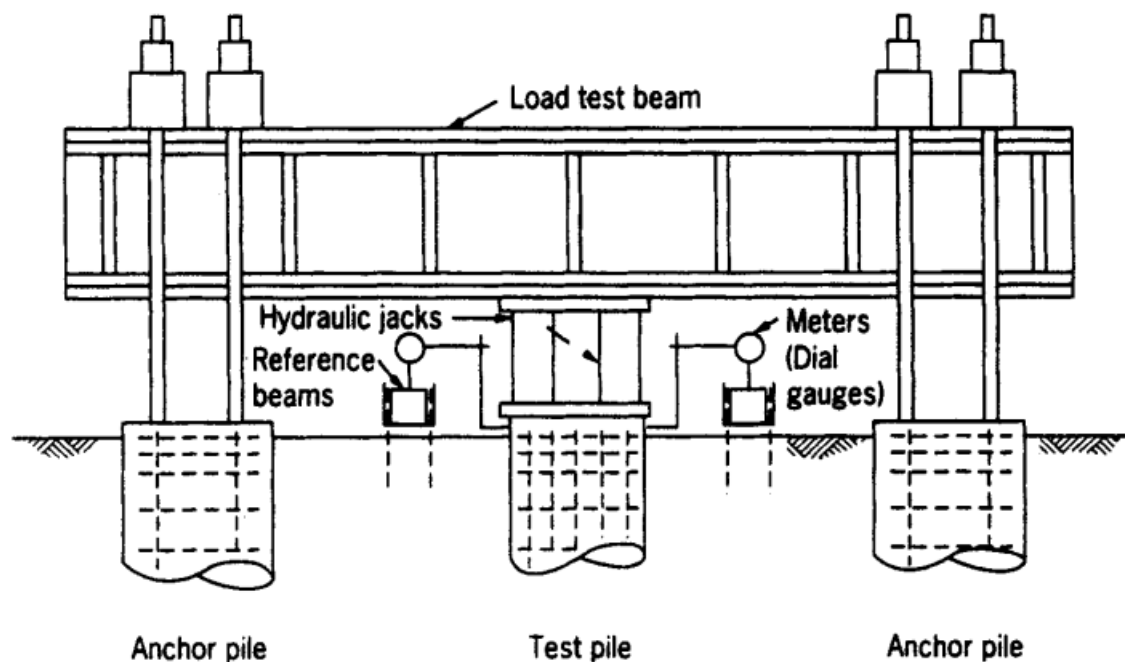


Figure 2.3: Typical setup for pile load test in compression. (Sharma et al., 1984).

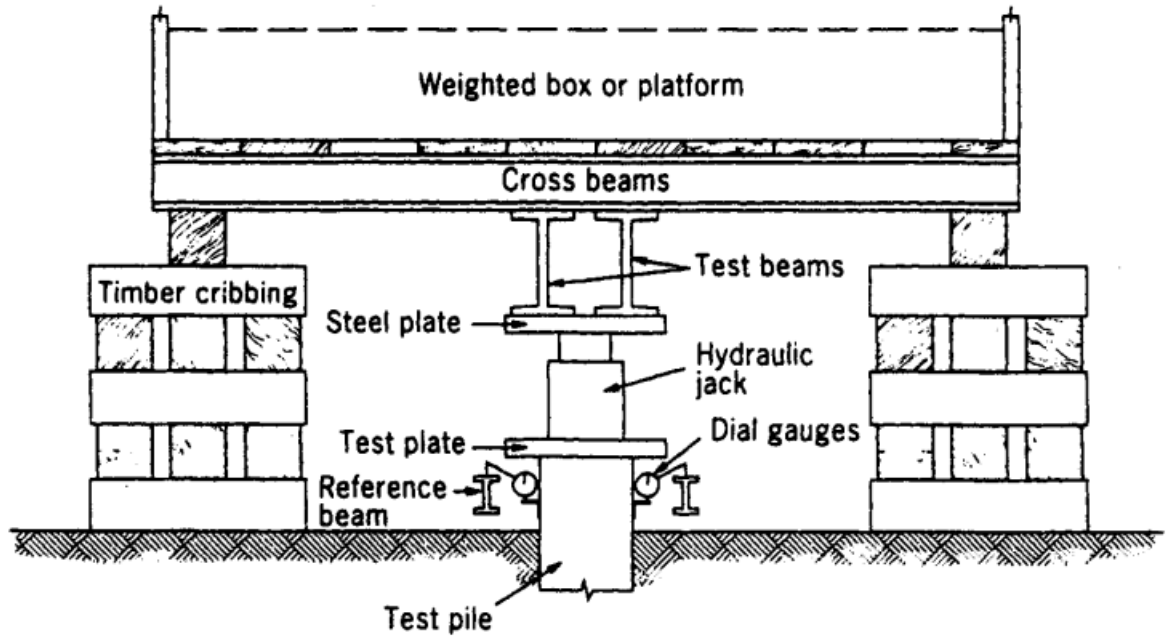


Figure 2.4: Typical setup for pile load test in compression (ASTM Institute, 1977).

2.8 Finite Element Method

The Finite Element Method (FEM) is a numerical approach commonly used to solve complex engineering and physical problems that are governed by partial differential equations (PDEs) (Zienkiewicz et al., 2005). The finite element method (FEM) is a valuable tool in modeling the load-deformation characteristics of piles subjected to axial loading (Johnson et al., 2001). Many studies have been carried out in the last few decades to investigate the properties of sands and clays (Dahal et al., 2018). The parameters that are frequently examined in this context include sand's mechanical properties, such as ϕ , E , ν , and ψ (Degago et al., 2010). FEM provides a great advantage in handling complex geometries, heterogeneous materials, and mixed boundary conditions that are difficult or impossible to solve analytically (Cook et al., 2001). The method involves several key steps, including discretization of the domain, element formulation, assembly of the global stiffness matrix, application of boundary conditions, and numerical solution (Zienkiewicz et al., 2005). Each element contributes to the global stiffness and load matrices based on its material and geometric properties, which are then solved to yield nodal displacements or other primary variables. From these results, secondary quantities such as stresses and strains can be computed (Reddy, 2006). Constitutive models simulate the mechanical behavior of soils in the field of FEM (Devkota & Dahal, 2022; Puri & Dahal, 2022; Regmi et al., 2021). The continuous development of FEM theory and computational techniques has established it as a

cornerstone of numerical modeling and simulation in scientific and engineering research (Zienkiewicz et al., 2005).

New numerical approaches have contributed greatly to the improvement of geotechnical engineering, allowing the detailed analysis of complex soil–structure interaction issues (Zienkiewicz et al., 2005). This latter part of the research, in particular, emphasizes the Finite Element Method (FEM), which has become one of the most widely employed methods to solve problems based on partial differential equations (PDEs) (Zienkiewicz et al., 2005). It is widely applied in slope stability assessment, foundation analysis, retaining structures, tunneling, excavation, and pile design. Because it discretizes the problem domain into smaller components, FEM enables engineers to model soil and structural behavior in many different ways when under different loading conditions. It also incorporates non-linear material characteristics and spatial variability of soil properties and makes the analytical results more reliable (Klaus-Jürgen Bathe, 1996).

Numerous studies have been performed on the behavior and performance of laterally loaded single piles and group piles. Plaxis-3D numerical analysis of laterally loaded piles is widely used to investigate the behavior of laterally loaded piles in a variety of research papers. These numerical models are increasingly popular as they can fairly accurately predict such phenomena as displacements, shear strength, and stresses of piles and types of foundation systems in different soils. Plaxis-3D has been extensively used for many applications in engineering, such as lateral load behavior and bearing capacity calculations.

This literature review focuses on evaluating numerical approaches for predicting horizontal displacement in sandy soils using Plaxis-3D. However, there is a lack of studies investigating its performance for piles embedded in layered soil conditions. Existing findings suggest that Plaxis-3D provides reasonably accurate results for common cases, but further research is necessary before it can be broadly applied in geotechnical engineering practice.

2.9 Site Description

The bridge project is situated over the Mahuli River in the Saptari district of Province 2 (Chainage 160+700). Numerous rivers flow from north to south along Nepal's East–West Highway in this region (Gupta & Dahal, 2023a).



Figure 2.5: Google map of site location.

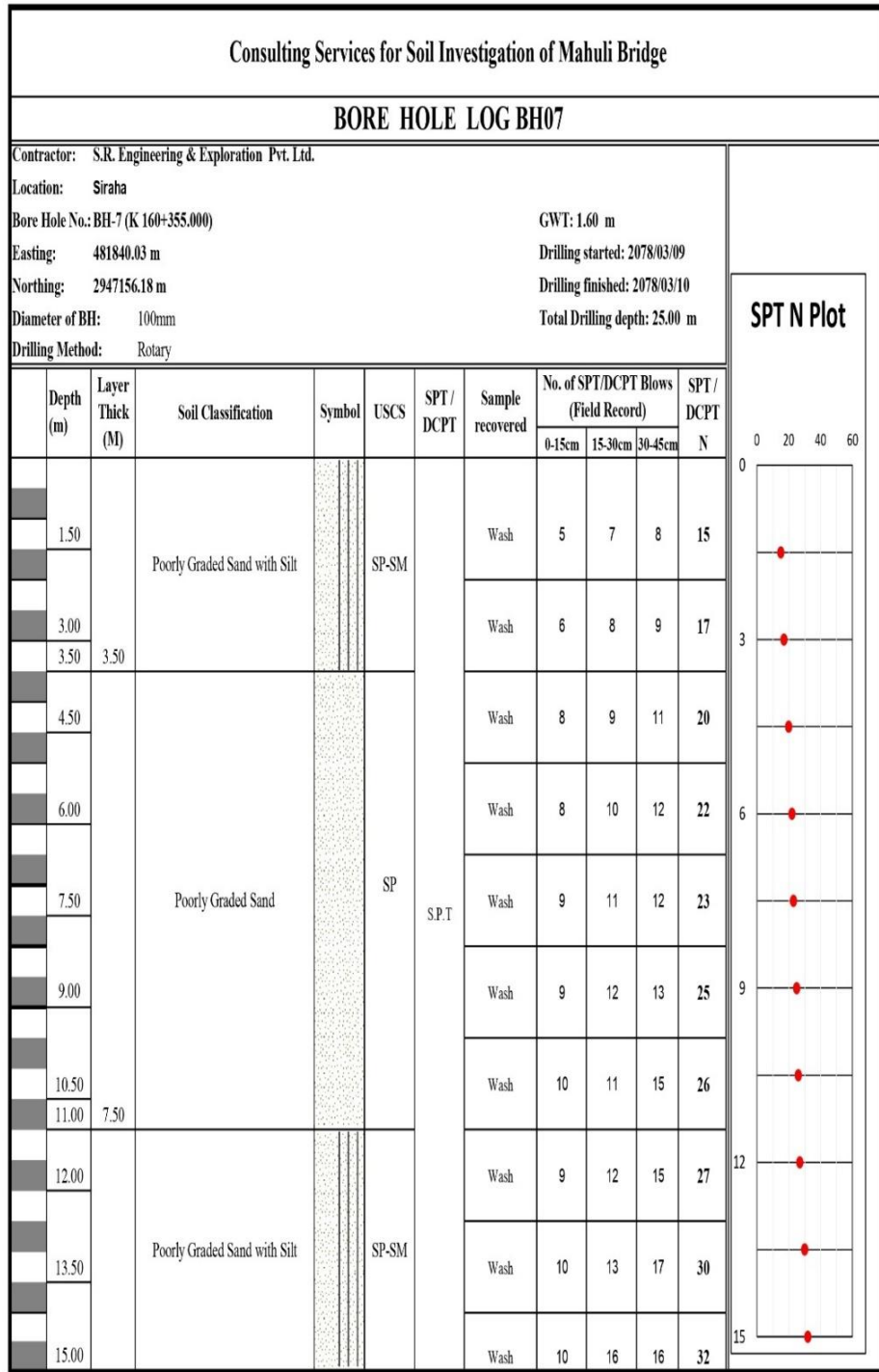
2.9.1 Geology of the site

The site is characterized by relatively flat terrain and is located in the eastern Terai region of Nepal. This area forms the northern extension of the Indo-Gangetic Plain and lies at an elevation of approximately 100–200 meters above sea level, with a subtropical climate. It extends from the foothills of the Siwalik range in the north to the Nepal–India border in the south, with a width ranging from about 10 to 50 km. The Terai can be further divided into three zones: the northern (Bhabar), central, and southern regions. In the northern part, near the mountain front, the soil primarily consists of coarse gravels that gradually transition into finer materials toward the south. The site is approximately located at coordinates 26.644797° E and 86.816281° N (Engineering, 2021), as illustrated in the referenced (Gupta & Dahal, 2023a).

2.9.2 Geo-mechanical Parameters

The type of soil is poorly graded sandy soil with silt. The soil is medium-dense sand with an average SPT value ranging from 15 to 39. The key parameters include a unit weight of soil of 18 KN/m³, and the value of cohesion is 0. The frictional angle value for the soil type is (30–32) degrees. The effective Poisson's ratio value is 0.28. The value of Young's modulus of elasticity varies with depth. Mahuli Khola Bridge was selected because it has sandy riverbed soil and pile foundations similar to those of many bridges constructed in Nepal. Also, field test data were available

for validation of my Plaxis-3D numerical model. Therefore, the study results apply to similar bridge foundations used in Nepal.



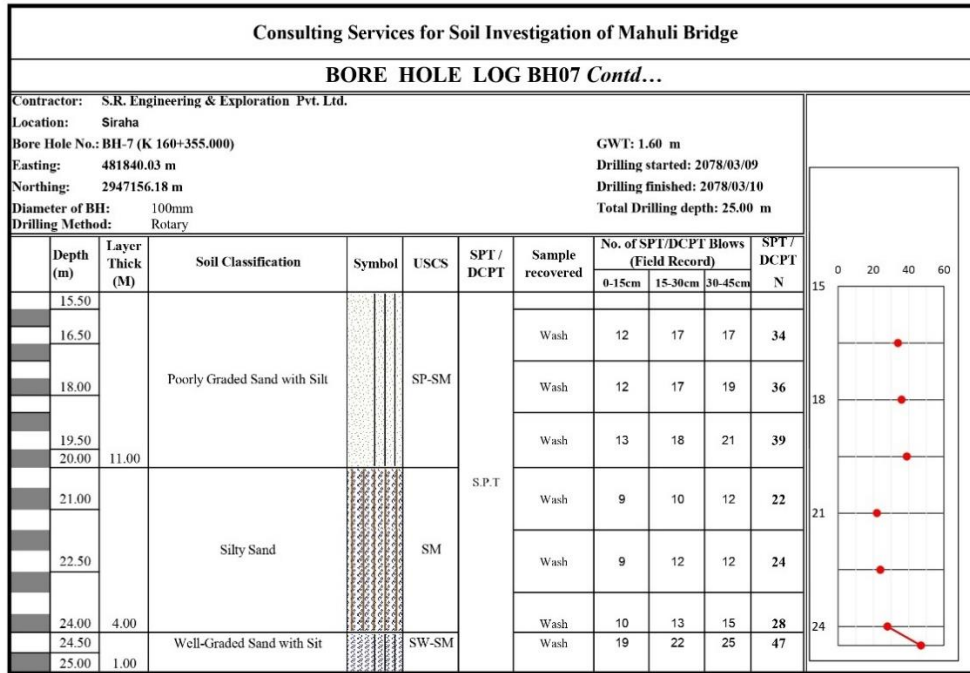





Figure 2.6: Borehole log sheet.

3 RESEARCH METHODOLOGY

The research technique for a thesis outlines the systematic framework for collecting, analyzing, and interpreting data. The process begins with establishing the research design, which may be qualitative, quantitative, or mixed methodologies, depending upon the research question. This section outlines sample methodologies, data collection tools, and analytical techniques, while considering ethical issues such as confidentiality and informed consent. The methodology seeks to facilitate the replication of the study and the evaluation of its validity and reliability. It incorporates a sequence of procedures, including literature study, field and laboratory studies, and the creation of numerical models, accompanied by comprehensive guidelines on the instruments and techniques employed. The methodology chapter enables readers to assess the research's trustworthiness, validity, and the thesis's subject matter.

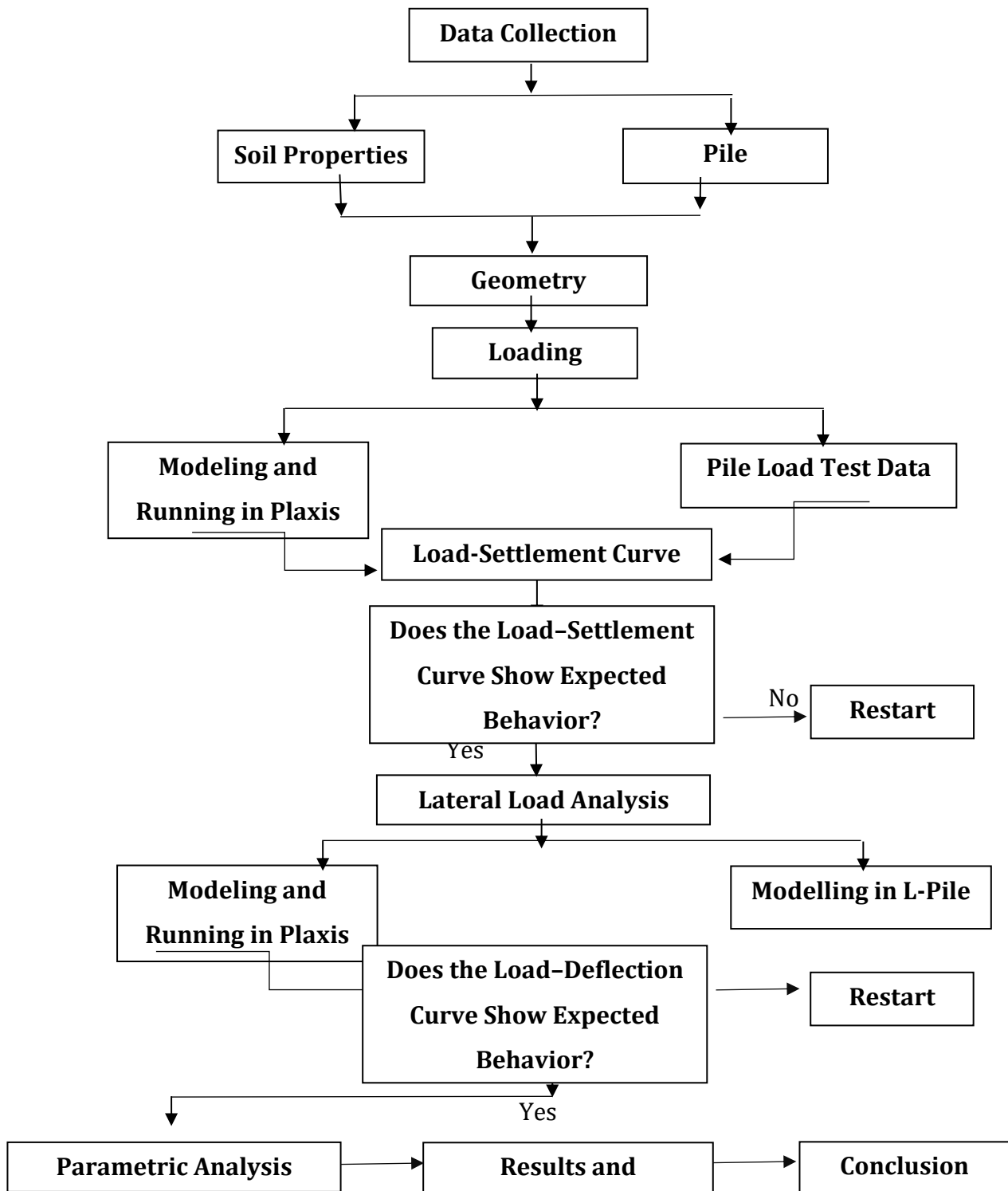


Figure 3.1: Conceptual framework of the study.

3.1 Geometry

The processing time for numerical analysis is significantly influenced by the model's dimensions and elemental composition (Garcia & De Albuquerque, 2018). Additionally, depending on the model's dimensions and element count, the

computational time needed for numerical analysis varies greatly (Nasasira Derrick, 2020). Therefore, selecting suitable boundary conditions is a critical aspect that has been emphasized in many research studies. As a result, the bottom edge of the model was fixed in all directions, while the side edges were limited in horizontal movement (Liyanapathirana et al., 2005).

The axisymmetric mesh of 10-node triangular elements is used to compute the model size (Brinkgreve, 2021). The size of the mesh was adopted from coarse to very fine to closely predict the field settlement value of the pile load test. Figure below shows that the five-layer sandy soil, each with different properties like unit weight, strength parameters, friction angle, and stiffness value, is defined in order to construct the geotechnical model. These five-layer soil strata have different thicknesses. The choice of the size of the model would minimize strain closer to the boundary in dimensions that would be smaller. Calculation time will increase as the geometry becomes larger. Thus, the dimension of the model was chosen as 20 m in length, 20 m in breadth, and 30 m in depth, to maximize the geometry of the model and computational time, as shown in the figure (Gupta & Dahal, 2023a).

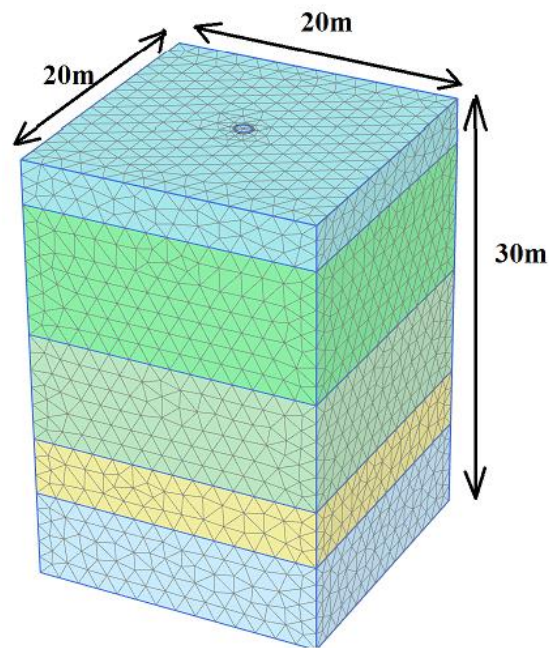


Figure 3.2: Mesh model of Plaxis-3D for a single pile.

3.1.1 Meshing

In Plaxis 3D, soil was discretized into 10-node tetrahedral elements, following the meshing procedure outlined in the Plaxis Reference Manual. Various mesh elements are applied to structural components and interface zones. Mesh

generation is a critical step in finite element analysis, as it directly affects both accuracy and computational efficiency. The mesh must be sufficiently refined to produce reliable results while remaining coarse enough to limit computation time. Plaxis-3D provides five standard mesh densities: very coarse, coarse, medium, fine, and very fine. While finer meshes take a bit more time and a better computer to achieve, the settlement prediction for the pile load test varies from very coarse to very fine meshes, depending on whether the mesh is refined (Derrick, 2020). The effects of changes in mesh size on the model results were analyzed. For elements with 15 nodes, the distribution of nodes is better, and the results are more accurate than for elements with six nodes or 10 nodes (Gupta & Dahal, 2023b). Mesh size affects the bearing pressure at a given settlement and vice versa (Nasasira Derrick, 2020). Therefore, the analysis is carried out with 10-node elements. However, educational Plaxis has only elements with 10 nodes. But 15 nodes bring better results. The finer the mesh, the better the settlement trend and prediction.

The geometric model had been prepared, as well as the subsequent process of meshing. The aim was to arrive at a refined, accurate and numerically stable calculation. To facilitate this, large quantities of soil elements were produced, in regular shapes to prevent excessive elongation and thinness. Elements should be regular-shaped and uniform, not elongated and/or thin, so that mesh quality was of utmost importance. It is critical to having such a method so that the numerical stability could be secured. To achieve the proper accuracy, the mesh granularity was selected to avoid the extreme of making it all very small and therefore resulting in the computation time being prolonged from the smallest elements. To preserve the quality of the mesh, we meticulously considered how to achieve a trade-off between accuracy and computational time. In the soil material element consisted of 10-node tetrahedral elements as shown in Figure 3-3, and in the embedded beam, three-node line elements were added to mimic behavior. For further improved accuracy, mesh was meshed with "Fine" distribution of the element and mesh refinement was performed. Refer to Figure 3-4 for the post-mesh generation geometric model.

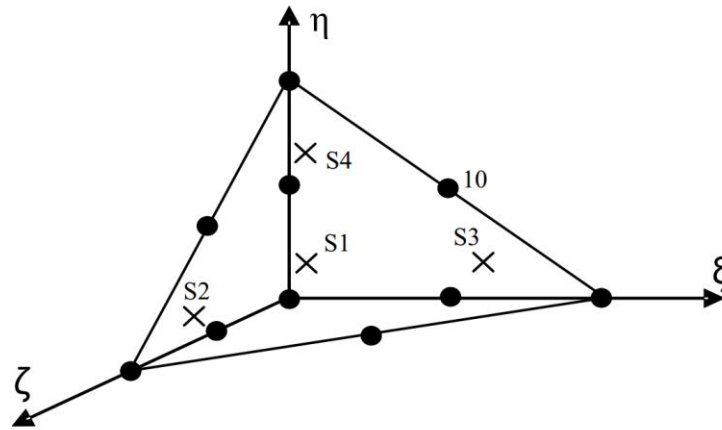


Figure 3.3: 3D soil elements (10-node tetrahedron) (Source: Plaxis).

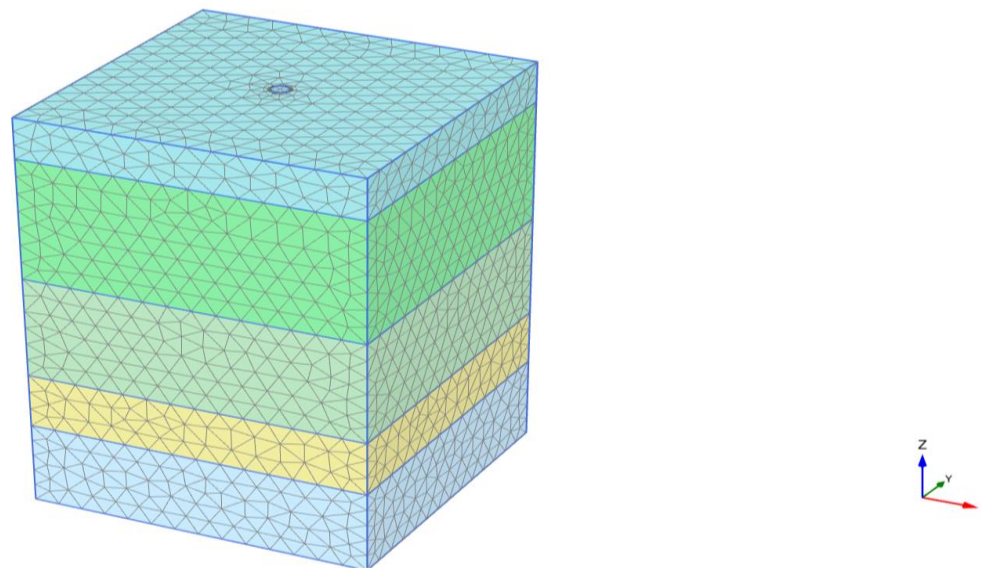


Figure 3.4: FEM model after meshing.

3.1.2 Boundary condition

In the Finite Element Method (FEM), the boundary conditions play an essential role in ensuring that the numerical model accurately represents the physical behavior of a structure or soil domain under external loads (Zienkiewicz et al., 2005). Boundary conditions define how the model interacts with its surroundings by specifying the constraints and loads at the boundaries of the computational domain (Cook et al., 2001).

Generally, boundary conditions in FEM are of two main types — essential (displacement) boundary conditions and natural (force) boundary conditions. The essential boundary conditions prescribe the displacement or rotation values (for

example, fixing or restricting movement at certain nodes), while natural boundary conditions define the external loads or stresses applied to the boundaries (Zienkiewicz et al., 2005).

For a geotechnical model, such as a pile–soil interaction in Plaxis-3D, the boundary conditions must prevent any artificial deformation that could distort the results. Typically, the bottom boundary of the soil domain is fully restrained in all directions ($U_x = U_y = U_z = 0$) to simulate the rigid base condition, ensuring no vertical or horizontal movement occurs at depth (Brinkgreve, 2021). The lateral boundaries are usually fixed in the horizontal directions perpendicular to their planes ($U_x = 0$ or $U_y = 0$), while allowing vertical movement to replicate natural soil behavior under loading.

The top boundary, representing the ground surface, is usually kept free to move and deform according to the applied loading, such as lateral or vertical pile loads. Incorrectly defined boundary conditions can lead to unrealistic results, such as over-constrained deformation or excessive stress concentrations, thereby compromising the model's accuracy (Bathe, 1996).

Therefore, the proper definition of boundary conditions ensures that the FEM model behaves realistically and provides reliable results that can be validated against experimental or field data.

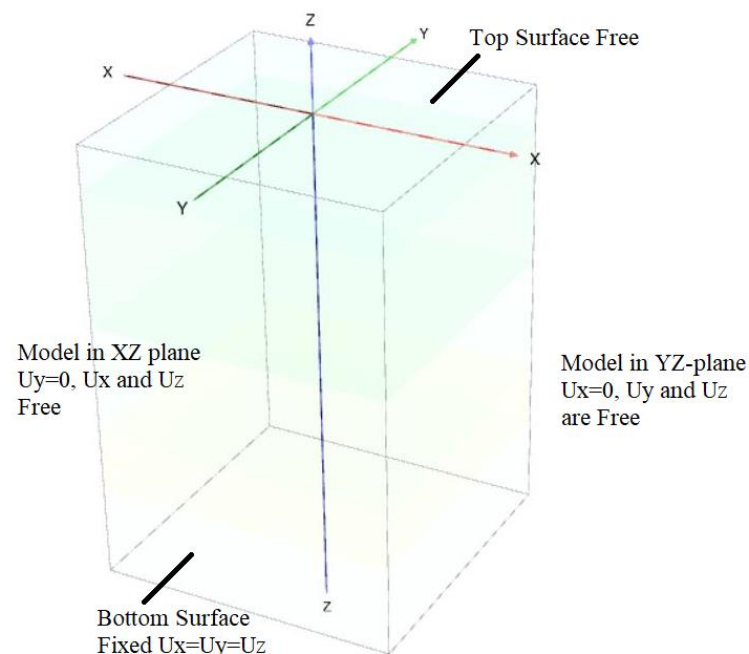


Figure 3.5: Boundary conditions.

3.1.3 Pile as volume beam element

In Plaxis-3D, piles can be represented as volume beams, which are structural elements that depict the pile as a three-dimensional beam immersed within the earth. The volume beam method enables the software to accurately model both bending and axial behavior of piles while realistically interacting with adjacent soil via soil-structure interface elements. In contrast to simple line beams, volume beams include distinct cross-sectional geometry (diameter or width), allowing Plaxis to incorporate pile stiffness (EI), shear deformation, and torsion in the analysis. This method works well for analysing piles under lateral loading, including pile groups, because it shows how stresses develop and change along the length of the pile more realistically. The interaction with the surrounding soil is represented using either interface elements or p - y curves, which depict the nonlinear soil resistance activated under lateral and axial loads. Additionally, volume beams in Plaxis-3D can incorporate material properties of concrete or steel, allowing for realistic elastic or elasto-plastic behavior during simulations. This makes them suitable for complex numerical analyses of individual piles and pile groups subjected to complex loading scenarios, including both axial and lateral forces.

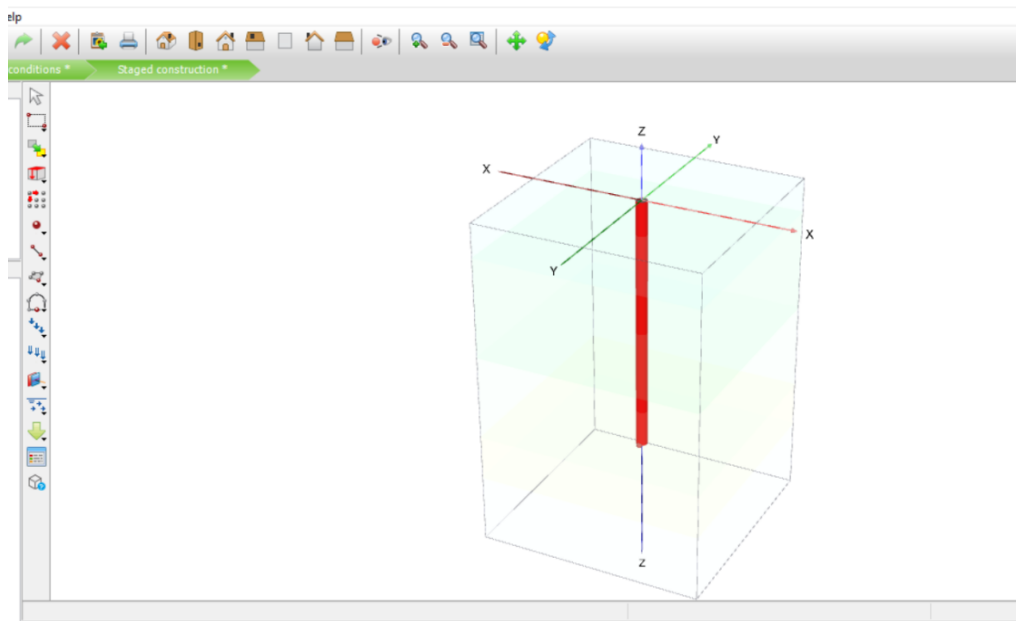


Figure 3.6: Pile as volume element.

The pile was modeled using a soil material dataset, but its parameters were adjusted to represent concrete behavior. In this study, M35 grade concrete was adopted for the pile. The modulus of elasticity of the concrete was estimated using the empirical relation as $E = 5000\sqrt{f_{ck}} = 29.58Gpa$.

Table 3.1: Material Data Set of the Plaxis volume pile (Gupta & Dahal, 2023a)

Parameter	Name	Value	Unit
Material model	-	Linear -elastic	-
Drainage type	-	Non-porous	-
Unit weight	γ	25	KN/m ³
Young's modulus	E	29.58	Gpa
Diameter	D	1	m
Length	L	22.77	m
Poisson's ratio	ν	0.15	-

3.2 Geo-mechanical Parameters

3.2.1 Data collection

The information used in this study was collected from both primary and secondary sources. Secondary data were obtained from previously published research, journal articles, and records maintained by relevant institutions and agencies. Primary data were collected directly through field visits, sampling of materials, and subsequent laboratory testing.

Borehole log data were used to define the soil layering, while additional soil parameters were obtained from the geotechnical report.

3.2.2 Soil exploration and properties

The type of exploration used at the site is a standard penetration test according to the site conditions (see Annex II). Most parameters were determined through laboratory and field investigations, with some relying on correlations (Kulhawy & Mayne, 1990b). The Standard Penetration Test (SPT) values were measured at different depths and are presented in the table below.

3.2.3 Sub-soil properties

Basic soil parameters, including bulk density and saturated density, were obtained from the relevant geotechnical report for the bridge site. The engineering

characteristics of the subsoil and the soil profile were then estimated using established correlations based on SPT (N). The following correlations were used:

1. Young's Modulus of Elasticity for sand

1.1. Bowles (1997)

Young's Modulus of Elasticity for sand for 55 % energy is given by $E = 7000 \times \sqrt{(N60 \times 60/55)} Kpa$

2. Angle of Internal Friction -: The angle of internal friction for the sand was adopted layer by layer from the geotechnical report, where it had been determined through laboratory direct shear tests (DST).

3. $\gamma_{sat} = (G_s + e) \times \gamma_w \div (1 + e)$

4. Correlation for poisson's ratio is given by

According to (Kulhawy & Mayne, 1990b)

$$\mu = 0.1 + 0.3 \times (\varphi - 25) \div 20$$

5. Dilatancy Angle for sand,

$$\omega = \varphi'_{peak} - 30$$

Where $\psi = 0$ for $\varphi'_{peak} < 30^\circ$

3.2.4 Mohr-Coulomb parameters

In FEM, the Mohr–Coulomb model represents the soil as an elastic–perfectly plastic material, requiring both elastic and plastic parameters to characterize its behavior (Brinkgreve, 2021). The elastic parameters include:

Young's modulus (E): defines the soil stiffness and controls deformation under loading.

Poisson's ratio (ν): represents the ratio of lateral to axial strain, indicating volumetric deformation tendencies.

The plastic parameters define the yield and flow behavior of soil after reaching the failure envelope:

Cohesion (c): It refers to the point where the failure envelope intersects the shear stress axis, indicating the material's shear strength when no normal stress is applied.

Friction angle (φ): slope of the failure envelope, representing the resistance due to interparticle friction.

Dilatancy angle (ψ): It describes the volume change (expansion or contraction) that occurs during plastic shearing, which in turn affects the form of the plastic potential surface.

In FEM software such as Plaxis-3D, these parameters are used to simulate the stress–strain relationship within each soil element. The Mohr–Coulomb model simplifies the nonlinear soil behavior while capturing the essential response under various loading conditions, such as lateral and vertical pile loading (Brinkgreve, 2021). Despite its simplicity, it provides sufficiently accurate results for many practical problems when the parameters are calibrated using laboratory or field test data (Duncan & Wright, 2005).

However, the Mohr–Coulomb model assumes constant stiffness and a perfectly plastic yield surface, which may not represent strain-dependent stiffness and hardening effects accurately. Therefore, for more refined analysis, advanced models like the Hardening Soil Model (HSM) may be used, but the Mohr–Coulomb model remains the most fundamental and widely applied for preliminary analysis and parametric studies. The Bowles (1997) method is used for Young's modulus of elasticity, as the model is validated using the Bowles (1997) method.

Table 3.2: Properties of the surrounding soil in Plaxis-3D (Gupta & Dahal, 2023a)

Layer	Depth	Material Type	Parameters			
			Drainage Type	Unit weight		Young Modulus (MPa)
				γ_{unsat} (kN/m ³)	γ_{sat} (kN/m ³)	Bowles (1997)
Layer 1	3	Sand	Drained	18	19.34	24220
Layer 2	9	Sand	Drained	18	18.08	33541
Layer 3	7.5	Sand	Drained	18	19.56	40927
Layer 4	4.5	Sand	Drained	18	19.8	34756

Layer 5	6	Sand	Drained	18	19.6	47940
------------	---	------	---------	----	------	-------

Layer	Parameters				
	SPT Value (N)	Poisson's Ratio	Cohesion (kN/m ²)	Friction Angle (degree)	Interface Interaction Factor
Layer 1	16	0.28	0	30	0.67
Layer 2	24	0.27	0	30	0.67
Layer 3	32	0.29	0	31	0.67
Layer 4	30	0.28	0	32	0.67
Layer 5	47	0.3	0	32	0.67

3.3 Pile and Pile Properties

A pile is a long, slender structural element made of concrete, steel, or timber that is driven or installed into the ground to transfer structural loads from a building or structure to deeper, more competent soil or rock layers. A deep foundation known as a bored pile is created by filling an open-drilled hole with fluid concrete transfer vertical loads from weak, surface soils to solid soil layers or rock at a predefined depth (Saran & Kumar, 2022). When a pile foundation is decided upon, it is necessary to compute the required pile cross-section and length based on the load from the superstructure, allowable stress in the pile material (usually a code value), and the in-situ soil properties (Bowles & Guo, 1996). It is generally accepted that a load test is the most reliable means of determining the actual pile capacity (Bowles,1997).

The test pile consisted of a cast-in-situ circular reinforced concrete element. Its key dimensions and material properties are presented in the table.

Table 3.3: Test pile properties (Gupta & Dahal, 2023a)

Materials	Concrete
Length (m)	22.77
Outer Diameter (m)	1
Young's Modulus (GPa)	29.58
Poisson's ratio	0.15

3.4 Routine Pile Load Test

The Mahuli Khola Bridge is located in the Saptari District, near the foothills of the Chure range in Nepal. Soil samples obtained during site investigation indicate the presence of sand with a minor proportion of silt, and the subsurface profile at the bridge site is predominantly composed of poorly graded (Gupta & Dahal, 2023a).

The bridge foundation consists of bored cast-in-situ piles with a diameter of 1000 mm, a length of 20 m, and concrete of grade M35. The designed allowable load capacity of each pile is 2160 kN. Routine pile load tests were carried out for each foundation at 1.5 times the allowable load, corresponding to 3250 kN (refer to Annex III). A routine load test was specifically conducted on a pier test pile of the Mahuli Khola Bridge in accordance with (IS 2911 (Part 4), 1985). The load-settlement data obtained from the test are presented in Annex 7.3, and the corresponding load-settlement curve is illustrated in the figure.

Table 3.4: Load-Settlement data of routine Pile Load Test

S.N.	Load (Ton)	Vertical Settlement (mm)
1	0	0
2	24.45	0.22
3	53.80	0.76
4	78.34	1.43
5	107.70	2.19
6	132.24	3.85
7	161.64	5.70
8	186.14	10.21
9	215.59	18.08

10	186.14	16.87
11	161.64	16.38
12	132.24	15.77
13	107.70	14.93
14	78.34	13.77
15	53.80	12.45
16	24.45	10.71
17	0	7.75

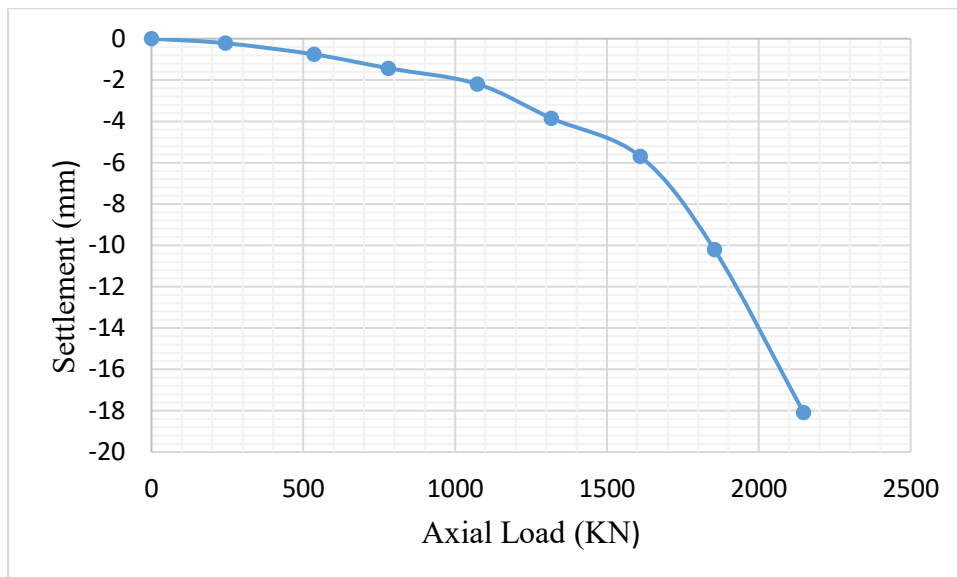


Figure 3.7: Pile load test curve at the field.

3.5 Lateral Load Analysis on Single Pile and Group Pile

For the analysis of laterally loaded pile deflection, a limit of 1% of the diameter (IRC:78,2014) is adopted for both single and group piles. This deflection criterion is frequently employed as the serviceability limit state for assessing the lateral load-bearing capacity of piles under horizontal loads. The lateral load capacity of pile groups is assessed by taking into account group interaction effects, which decrease the resistance provided by individual piles due to the overlap of soil stress zones. The distribution of lateral loads among piles is dependent upon their placement within the group, generally classified as leading, middle, and trailing piles. Leading piles typically experience greater soil resistance than trailing piles due to soil shadowing effects.

3.6 Finite Element Method

The Finite Element Method (FEM) is a computational technique widely used to obtain approximate solutions for complex engineering problems (Bathe, 1996; Zienkiewicz et al., 2005). In this method, the governing equations of a system are represented in a piecewise manner over smaller regions of the domain (Zienkiewicz et al., 2005). These components can be combined in many different ways to represent very large domains (V Jagota, 2013). The numerical analysis is based on the finite element method (FEM), an advanced method that can take into account most of the factors involved (Sert, 2003). In Finite Element Method analysis, problems are often simplified to two dimensions, where each node typically has two displacement degrees of freedom. This allows engineers to model a representative section of the domain efficiently. However, most geotechnical problems are inherently three-dimensional, and while plane strain or axisymmetric assumptions may be reasonable in some cases, certain situations require full three-dimensional modeling for accurate results (Brinkgreve, 2021; David V. Griffiths et al., 1999; Reddy, 2006). This means that three displacement components must be considered, and all three-dimensional geometry must be considered (Potts & Zdravković, 2001).

3.7 Numerical Analysis

Examining algorithms that use numerical approximations to solve mathematical analysis problems is known as numerical analysis (Kendall E. Atkinson, 1989). The analysis for this study uses the previously mentioned soil constitutive parameters for the MC model; the drainage condition is assumed to be drained because of the soil's notable high permeability, and the pile is modeled using linear elastic material (Gupta & Dahal, 2023a).

According to the Plaxis Connect Edition V21.01 Material Models Manual, Plaxis-3D is used in this study for both modeling and analysis (Brinkgreve, 2021). To verify the accuracy of the model, the results obtained from numerical simulations are compared with data from field pile load tests. Numerical analysis involves the use of computational methods to approximate solutions to mathematical problems, especially those dealing with continuous variables. In sandy soils, the modulus of elasticity (E) can be estimated from SPT values using correlations proposed by different researchers (Gupta & Dahal, 2023a).

Other parameters, such as the friction angle and Poisson's ratio (ν), are evaluated using correlations provided by (Kulhawy & Mayne, 1990a).

The geometry of the model is created, and soil properties along with the pile properties parameters are included in the Plaxis-3D software for numerical analysis. After the modeling mesh is generated, a fine mesh is used for better results and outcomes. The construction stage tab of Plaxis-3D divides the geometric model into several project phases. Each phase activates the soil and structures according to the requirements. The calculation of the initial stress field for the initial geometry configuration by the K0 procedure automatically defines the first calculation phase (the initial phase) (Brinkgreve, 2021). Subsequent phases of the calculation are defined manually by turning on the corresponding geometry and structure after the first phase. In each construction stage, the lateral deflection of 1% of the diameter is applied according to the condition for single pile and different pile group arrangements. Node points and stress points were selected at the interested location for the visualization of displacement and stress-strain parameters during and after the numerical calculation.

3.8 L-pile Software

L-pile is a popular specialized computer application that uses the p-y approach to analyze how piles respond to lateral loads. L-Pile software models the pile as a beam on an elastic or nonlinear foundation, dividing it into finite elements along its length. For each component, L-Pile employs iterative numerical methods to satisfy equilibrium between the applied lateral load and the soil resistance. A predefined lateral deflection criterion (e.g., 1% of pile diameter as per IRC:78-2014) is established as the permissible limit. The software incrementally increases the lateral load until the pile head or any point along its length reaches this deflection limit, thereby determining the ultimate lateral load capacity corresponding to the specified deflection. L-Pile computes slope, shear, and moment at each depth by solving the governing differential equation of a beam on elastic foundation $EI \frac{d^4y}{dx^4} + p(y)=0$, where EI is the pile stiffness, y is the lateral pile deflection, and p is the soil reaction (Isenhower et al., n.d.) .

4 RESULTS AND DISCUSSION

The numerical analysis of a pile load test for sandy soils was carried out by the Plaxis-3D software. The goal is to simulate and understand the behavior of different pile properties and the group effect under lateral loading on the pile and soil. The result of this analysis provides useful information for laterally loaded pile performance and capacity when they are placed into sandy soil layers. Following the analysis of the model FEM, the resultant data of the forces in the structures such as lateral force and lateral load capacity were extracted and expressed graphically. Parameters included here such as modulus of elasticity of soil, interface interaction factors between piles and soils (R_{inter}), variation in water level fluctuations, variation in diameter, and variation in length were taken into consideration in this study. For the group effect analysis pile spacing of 2D, 3D, 4D, 5D and 10D for arrangement 2×2 is considered and along with that pile group arrangement of 2×2, 2×3, 2×4, 2×5, 2×10, 3×2, 3×3, 3×4, 3×5, 3×10, 4×2, 4×3, 4×4, 4×5, 4×10, 5×2, 5×3, 5×4, 5×10, 10×2, 10×3, 10×4, 10×5 and 10×10 for spacing 3D, 5D and 7D is analyzed and p-multiplier effect is studied. The results of the different conditions are described in the following headings below.

4.1 Model Validation of Plaxis-3D Model Using Field Load Test Data

Model validation is a systematic procedure used to assess whether a model reliably represents the behavior of a given system. A comparison of the model's outputs with data gathered from experiments or field testing constitutes this validation process (Feng et al., 2017). Validation is the process of determining how well a model represents reality (Brinkgreve, 2021).

In this study, load–settlement data from field pile load tests were used to calibrate the PLAXIS 3D model. Multiple analyses were performed to examine how settlement changes when different empirical correlations are applied. The Mohr–Coulomb (MC) model was adopted in PLAXIS 3D for the simulations. Here, the modulus of elasticity E values are adapted from FHWA-IF-02-034[Webb (1969), Chaplin (1963), Papadopoulos (1982), Bowles (1996), Kulhawy and Mayne (1990)], and interface strength ranges from R_{inter} (0.5-1.0). The results are interpreted graphically in the figure, which shows that the simulated field pile settlement and the MC model's predictions satisfactorily align.

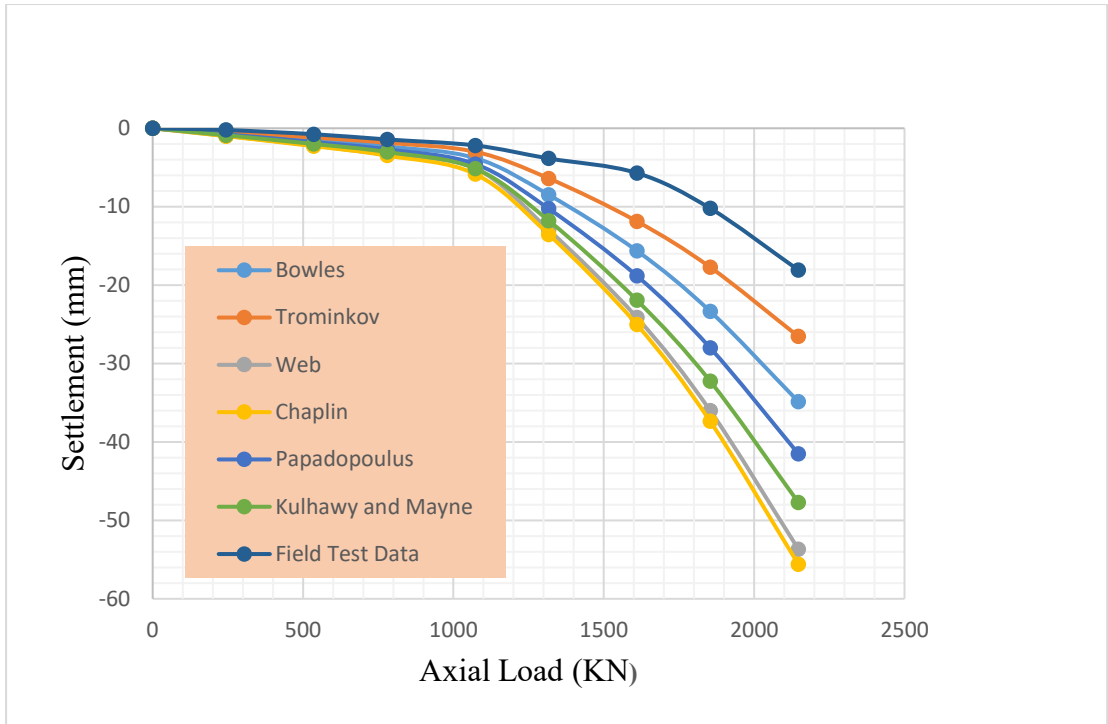


Figure 4.1: Load vs settlement for $R_{inter}=0.5$.

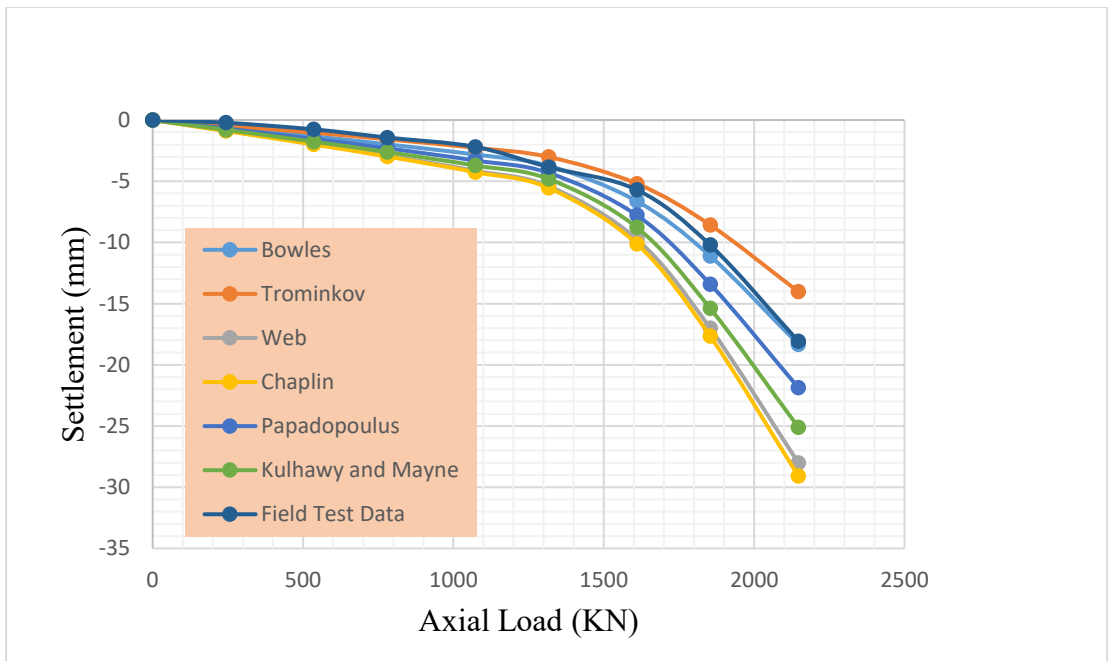


Figure 4.2: Load vs settlement for $R_{inter}=0.67$.

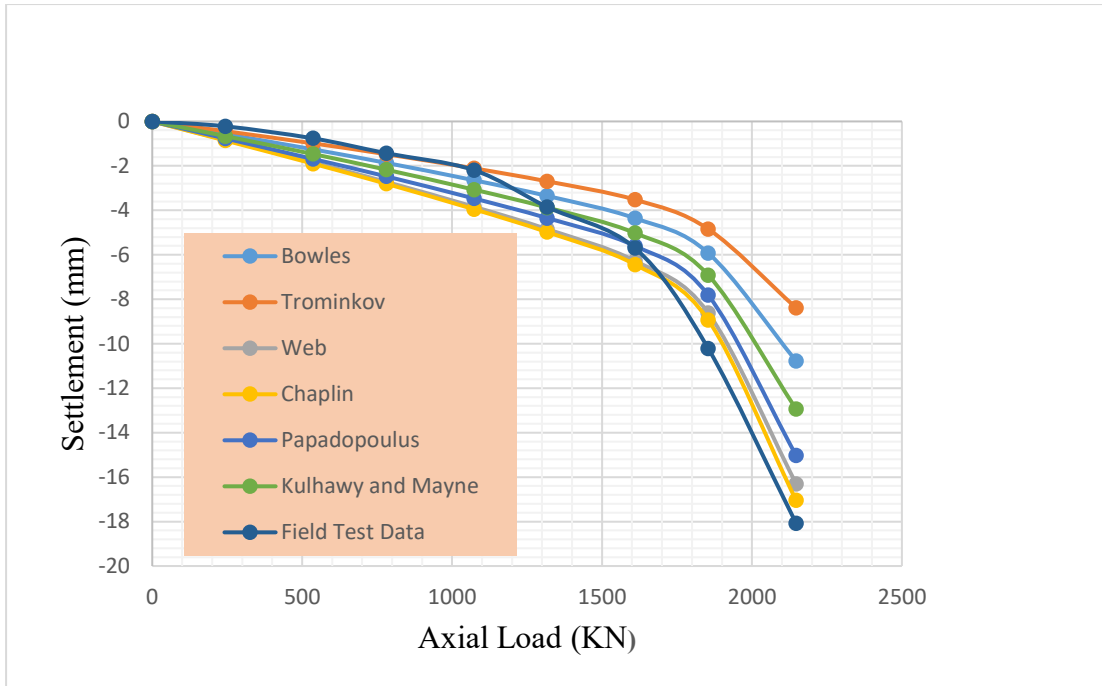


Figure 4.3: Load vs settlement for $R_{inter}=0.8$.

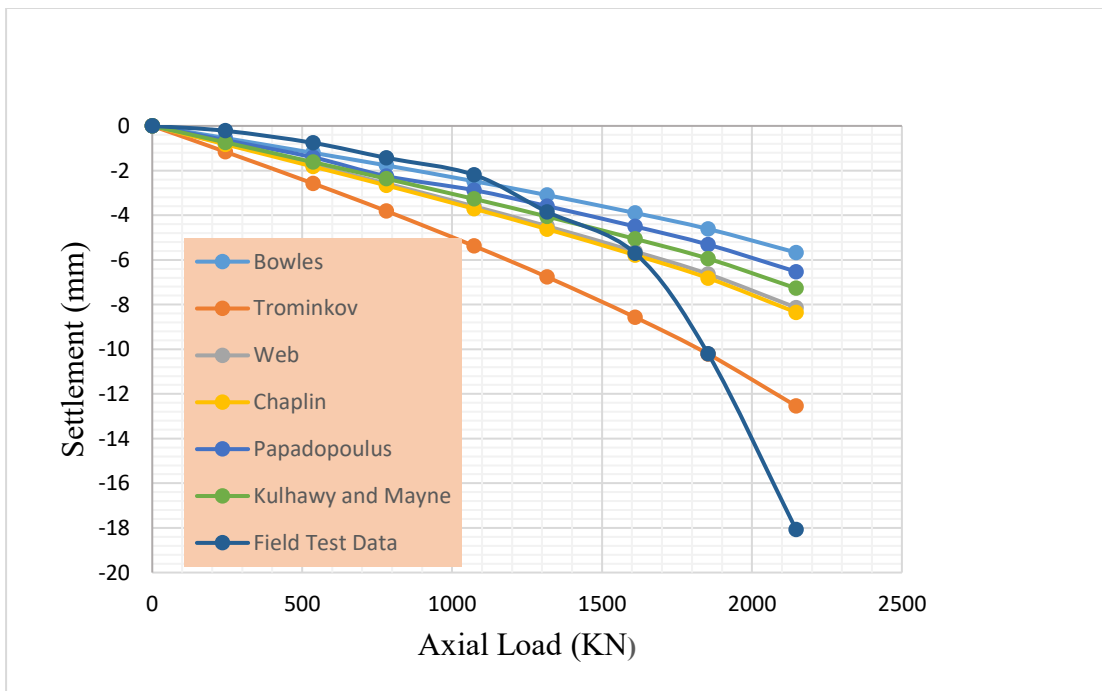


Figure 4.4: Load vs settlement for $R_{inter}=1.0$.

From the above analysis, the interface strength $R_{inter}=0.67$ and the Bowles modulus of elasticity give a close prediction with the field settlement value. The Webb (1969) and Chaplin (1963) give excessive settlement compared to the field

value, and with an increase in interface strength, the settlement value is also increased.

The model was calibrated using vertical load test data, which ensured realistic soil stiffness and strength parameters. Although lateral load test data were not available for direct validation, the predicted lateral load–deflection curves are still reliable because the same soil parameters control lateral resistance in sandy soil. However, the results should be interpreted as calibrated predictions rather than fully field-validated lateral behavior.

4.2 Lateral Load Response of a Single Pile Using Plaxis-3D

After the model is calibrated by field settlement value and Plaxis-3D results for axial loading, the same model is analyzed by applying the deflection criteria limit for lateral deflection, i.e., 1% of diameter for lateral load capacity from IRC:78 2014. The model with interface strength 0.67 and Bowles modulus of elasticity is used for further lateral load analysis.

4.2.1 Effect of meshing on the model

Mesh in Plaxis-3D works by discretizing the 3D geometry into finite tetrahedral elements, automatically creating a 10-node tetrahedral mesh based on global coarseness settings (very coarse to very fine). It calculates stress and deformation at these nodal points, allowing for local refinement around structures or sharp corners to improve accuracy in high-stress areas. In the Finite Element Method (FEM), meshing refers to the process of discretizing a continuous domain into smaller finite elements for numerical analysis (Zienkiewicz et al., 2005). The quality, size, and type of mesh elements have a significant influence on the accuracy, convergence, and computational efficiency of the model (Cook et al., 2002). Figure illustrates that with finer meshing, the lateral load capacity increases and gives an accurate result. The analysis is done for a diameter of 1.0m where the criteria of deflection limit 1% of the diameter is adopted. Here, the lateral load capacity increases from very coarse to fine and slightly decreases from fine to very fine. Hence, a finer mesh size gives a more accurate result (Gupta & Dahal, 2023a).

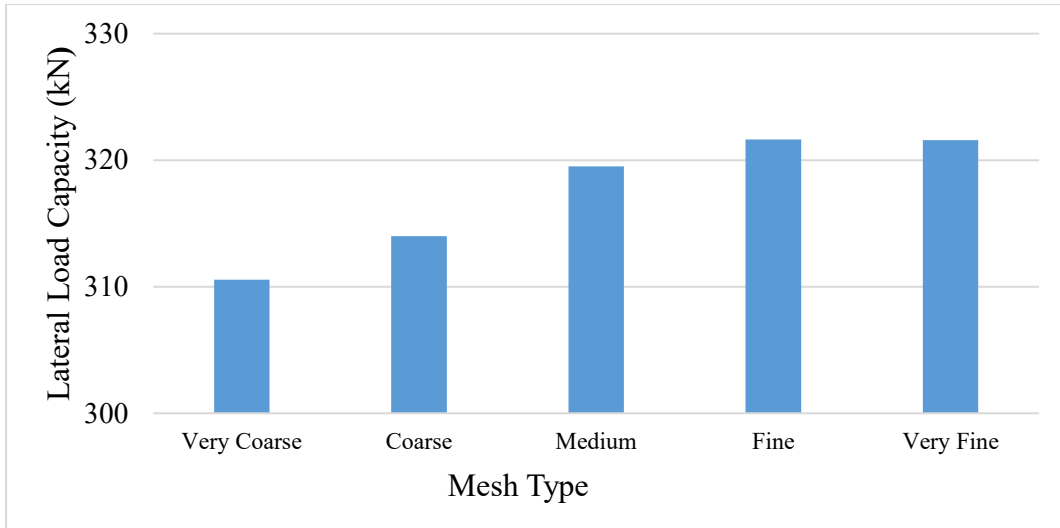


Figure 4.5: Effect of meshing on displacement

4.2.2 Effect of the interface interaction factors R_{inter}

The lateral load versus lateral displacement for different interface strength shown in the figure below. The curve plotted for different interface R_{inter} value ranges from (0.5-1.0) indicates that the lateral load capacity increases with an increase in interface strength. The increase in interface strength enhances the shear resistance of the soil pile system and increases the soil pile bonding, which helps to enhance the lateral load capacity of the pile.

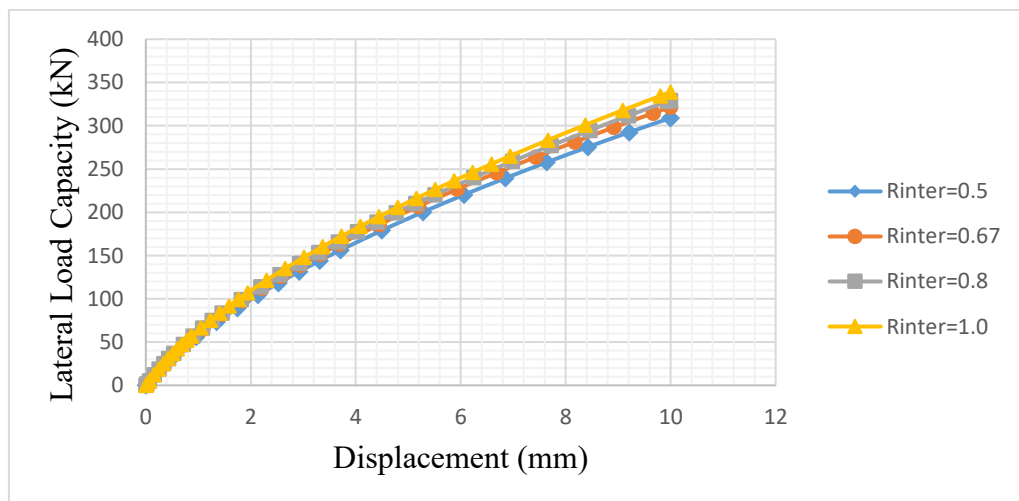


Figure 4.6: Load vs displacement for interface interaction factor

4.2.3 Effect of diameter

The diameter of a pile is essential in assessing its lateral load capacity. An increase in pile diameter results in increased lateral load capacity, resulting in the simultaneous increase in flexural rigidity (EI) and an increased soil-pile

interaction area (LC Reese et.al.,2025). The ultimate lateral capacity is directly proportional to pile diameter in both cohesive and cohesionless soils, as larger diameters generate greater soil resistance (Broms, 1964).

Parametric analysis examined how varying pile diameters influenced lateral displacement, aligning with trends reported in Marjanović et al. (2020). The lateral load versus Lateral displacement for increasing diameter from 0.8 m to 2.0 m is shown in the figure. The curve plotted below for varying diameter of pile with applied lateral displacement for deflection limit criteria 1% of diameter versus lateral load capacity, which illustrates that with an increase in diameter from 11% to 25%, there is an increase in lateral load capacity from 32% to 72%. Here, the increase in diameter increases the value of the moment of inertia; hence, the lateral load capacity increases.

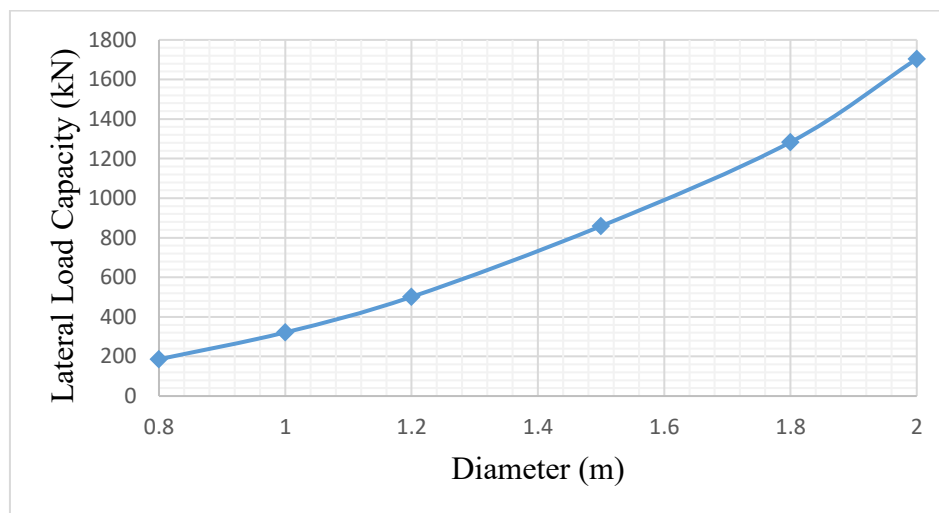


Figure 4.7: Load vs displacement for varying diameter.

4.2.4 Effect of pile length

The numerical findings from the lateral load analysis demonstrate that the lateral load capacity of piles increases with embedment depth until a certain limit, beyond which any increases in pile length do not significantly increase lateral resistance. This behavior was seen at embedment depths of roughly 12 m for 0.8 m diameter piles, 15 m for 1.0 m diameter piles, 18 m for 1.2 m diameter piles, 23 m for 1.5 m diameter piles, 30 m for 2.0 m diameter piles, and 35 m for 2.5 m diameter piles in the current investigation. Researchers confirmed that a critical pile length exists beyond which further increase in length does not affect pile head response under lateral loading (Liu et al., 2025). It is also observed that the critical length increases with pile diameter due to increased flexural rigidity (EI), allowing deeper mobilization of soil resistance (Wei et al., 2024).

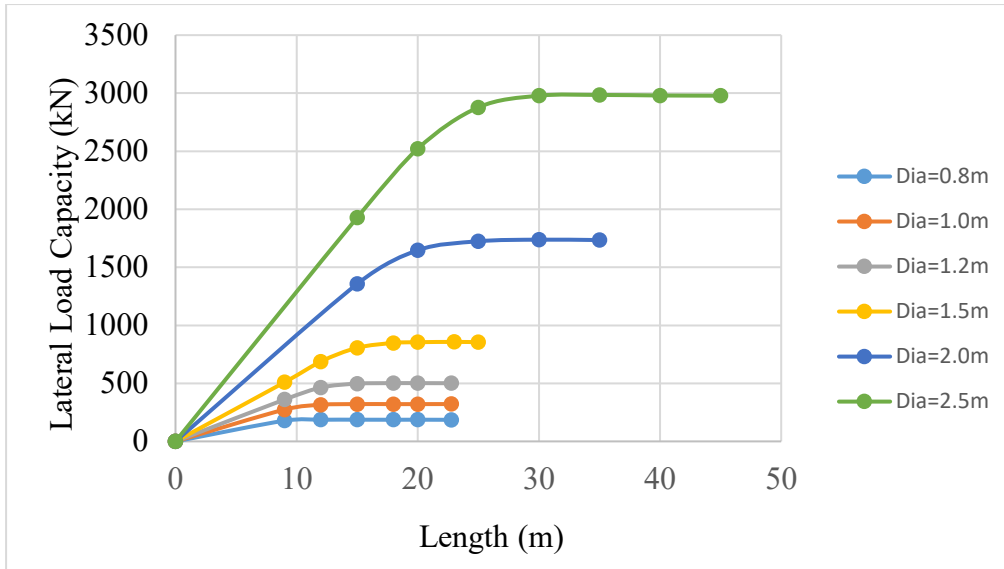


Figure 4.8: Load vs displacement for varying length and varying diameter.

4.2.5 Effect of water level variations

The groundwater level has a significant influence on pile performance during load testing. Water within the soil alters both the load-carrying capacity and the settlement behavior of the pile. When the water table is near the ground surface, the effective stress in the soil decreases, which generally leads to reduced soil strength and lower resistance against applied loads. In addition, groundwater can reduce friction along the pile–soil interface by providing a lubricating effect, thereby lowering shaft resistance. It also alters the effective stress within the soil and can increase its compressibility, further affecting pile performance.

The rise in water table increases the lateral load capacity, and there is no change in the value of displacement of the water table above ground level, as shown in the figure.

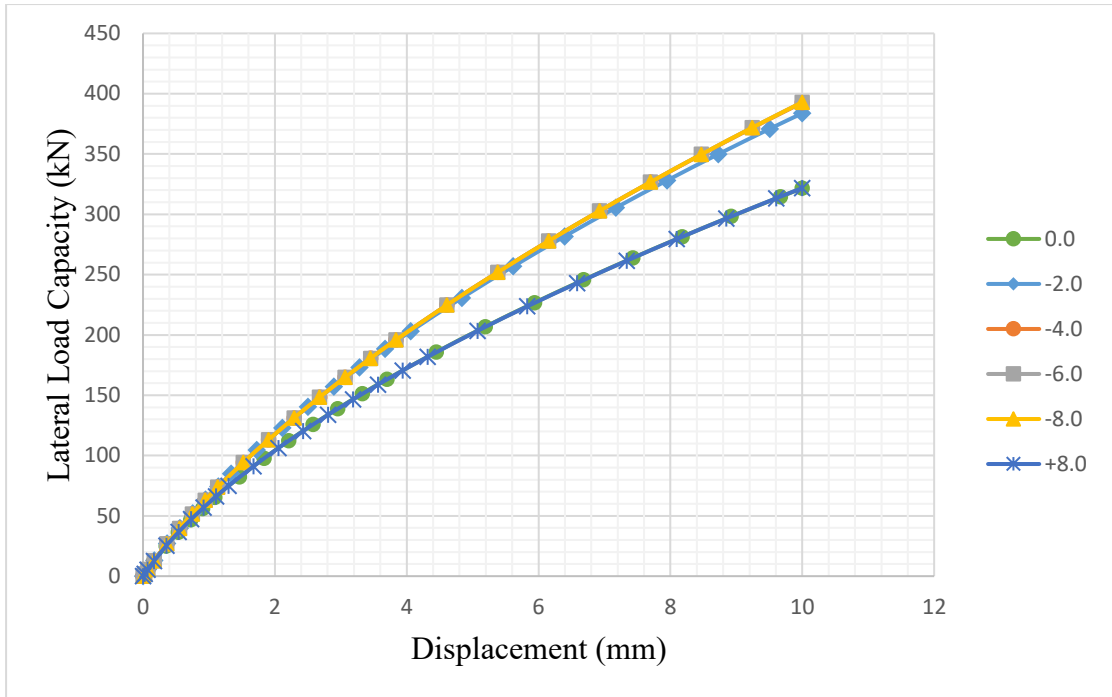


Figure 4.9: Variation of displacement versus water table

4.2.6 Verification of Plaxis-3D results with L-Pile

The L-Pile program represents a pile as a beam supported by an elastic or nonlinear soil medium, discretizing it into finite elements along its length. The model is analyzed in L-pile software and Plaxis-3D with increasing diameter from 0.8m to 2.0m and considering the deflection limit 1% of the diameter from IRC:78 2014. The figure below shows that the results from the L-pile are satisfactory and align with the results from the Plaxis-3D outcome. Hence, the model is validated using L-pile software, as L-pile is a widely used and accepted software in research.

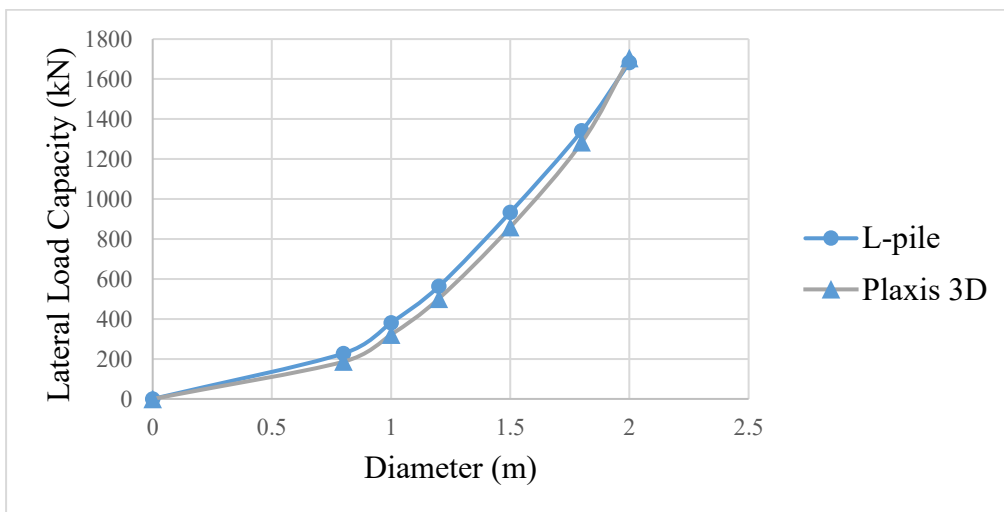


Figure 4.10: Variation of lateral load capacity vs diameter for L-pile.

4.3 Lateral Load Behaviour of Group Pile Analysis

Group Pile analysis is done for different numbers of piles with different pile group arrangements. The lateral displacement of 10mm is applied to the plate in Plaxis-3D for analysis. The adopted lateral displacement is 1% of the diameter. For the group analysis, the lateral deflection for different pile spacing and the lateral force carried by each pile are studied. Also, the p-multiplier effect for each leading, trailing, and middle pile is studied for different pile numbers with different arrangements.

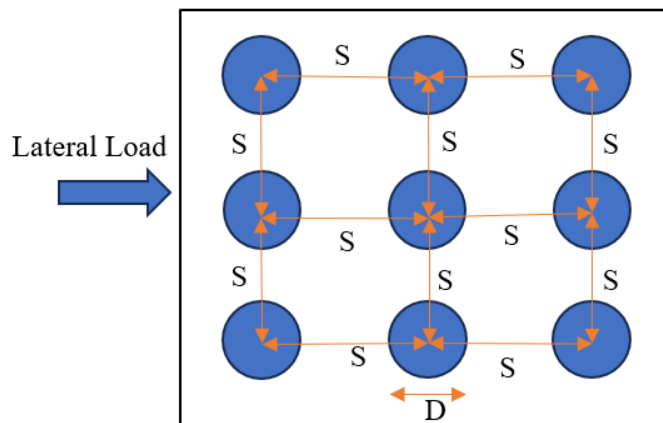


Figure 4.11: Pile group arrangement for 3×3 pile.

4.3.1 Effect of pile spacing

The Spacing between the piles has a significant influence on how the pile group responds to the applied load. When piles are closely spaced, their stress zones in the surrounding soil overlap, leading to interaction effects under lateral loading. This results in group behavior similar to a stronger soil-pile system, increasing overall lateral deflections and bending moments as compared to isolated single piles. The Pile spacing used in this study is 2D, 3D, 4D, 5D, and 10D for a 2×2 group pile. The load displacement curve of different pile spacing for a diameter of 1.0m and a length of 22.77m long pile in sandy soil is presented in the figure below. Under the same applied lateral loads, the pile spacing 2d gives more deflection than the pile spacing 5D and 10D.

The numerical analysis confirmed that pile groups exhibited lower lateral resistance than single piles, consistent with prior experimental findings on shadowing effects (Brown et al., 1988; M. C. McVay et al., 2000). Increasing the space between piles in a pile group often reduces the lateral displacement of

individual piles under the same applied lateral loads, as increased spacing reduces the extent of soil–structure interaction and the overlapping stress zones among neighboring piles. Research indicates that when pile spacing is small (e.g., less than about 6 D, where D represents pile diameter), the stress fields around adjacent piles exhibit significant interaction, resulting in greater lateral deflections than those observed in isolated single piles subjected to similar loads (Abbas Al-Shamary et al., 2018). As the spacing increases, the interaction effects decrease, and the lateral reaction of each pile is equivalent to that of an isolated pile, leading to reduced overall lateral displacements (Elhakim et al., 2016).

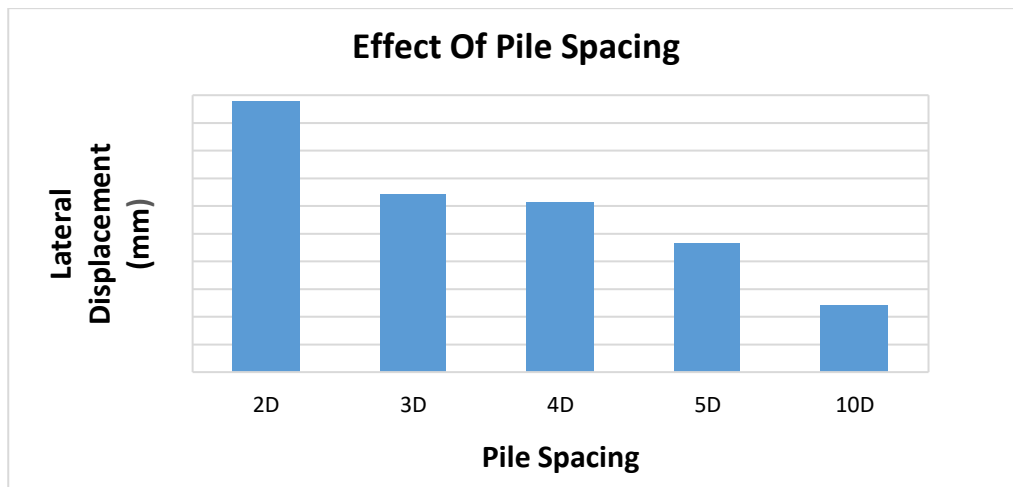


Figure 4.12: Variation of lateral displacement versus pile spacing.

4.3.2 Load-sharing behavior of piles in groups

The effect of different parameters on the load-deflection response of the loaded piles and the load distribution within pile groups with fixed heads was evaluated through running parametric studies. The table below shows the different pile arrangements and the results of their analysis in Plaxis-3D. Here the shear force carried by each pile is illustrated which shows that lead row carries more shear force than the preceding row as mainly due to soil–pile–pile interaction and the shadowing effect. The soil in front of the leading piles is initially intact, which provides greater resistance, resulting in higher shear force and bending moment in the leading piles (Brown et al., 1988).

4.3.3 Effect of pile spacing on shear force distribution

The results of the parametric analysis indicate that pile spacing has a strong influence on how shear forces are distributed within a pile group. When the spacing is small (around 3D), interaction between adjacent piles causes their stress zones to overlap, which limits the amount of soil resistance available to the

piles behind. Consequently, the front piles carry a much larger portion of the applied lateral load.

As the spacing expands from 3D to 5D and then to 7D, the contact among piles diminishes, resulting in a more uniform distribution of shear stress across the rows. This happens because increased spacing reduces the overlap of passive resistance zones surrounding neighboring piles, allowing each pile to utilize greater independent soil resistance. So, increasing spacing enhances load distribution efficiency within the pile group and improves the lateral performance of trailing piles.

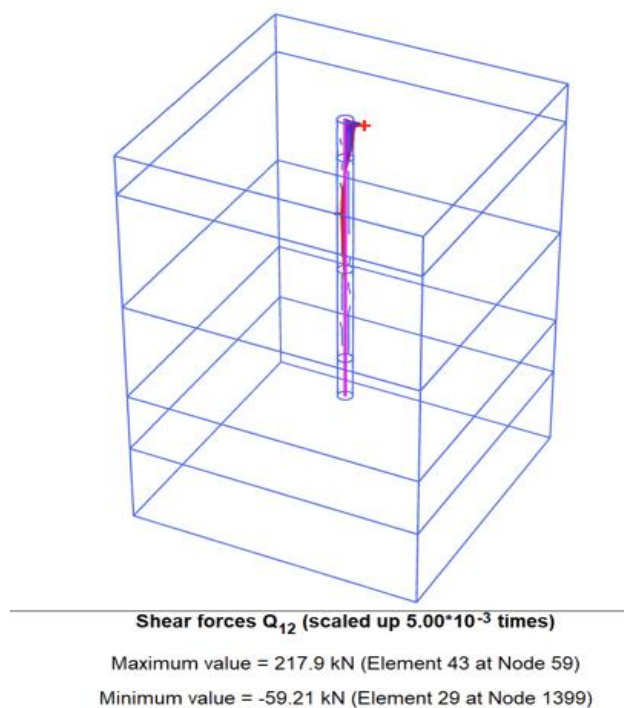


Figure 4.13: Shear force single pile.

Shear Force Single Pile = 217.9 kN

Table 4.1: Average shear force for each row pile in the group pile for spacing 3D

Pile Arrangement	Lead Row	2nd Row	3rd Row	4th Row	5th Row	6th Row	7th Row	8th Row	9th Row	10th Row
2×2	164.95	138.35								
2×3	166.45	136.45	128.30							
2×4	167.55	137.15	122.55	120.45						
2×5	168.70	137.50	123.60	113.95	115.50					
2×10	172.15	138.50	124.55	115.70	109.65	106.15	104.25	102.15	100.30	106.75
3×2	149.10	124.53								
3×3	149.93	119.37	110.98							
3×4	150.57	119.20	103.09	100.47						
3×5	152.10	120.43	103.73	94.25	94.52					
3×10	156.70	121.60	105.14	94.70	88.65	88.65	85.02	81.36	82.74	93.00
4×2	140.15	115.63								
4×3	140.53	109.66	99.69							
4×4	141.65	109.32	91.03	88.49						
4×5	143.30	111.23	93.12	80.83	82.17					

4×10	148.65	112.77	95.44	84.89	78.75	74.57	71.20	68.06	65.39	72.58
5×2	134.26	110.53								
5×3	133.02	103.01	92.51							
5×4	135.02	102.92	84.46	80.86						
5×5	137.60	104.68	85.85	74.38	74.52					
5×10	162.16	115.57	94.60	82.24	75.03	70.76	67.55	64.45	61.97	69.45
10×2	121.01	98.46								
10×3	119.34	88.62	77.40							
10×4	126.68	91.49	69.10	64.16						
10×5	133.78	93.41	71.97	56.25	56.23					
10×10	135.22	98.02	78.09	65.50	57.21	51.66	46.86	41.74	37.87	45.30

Table 4.2: Average shear force for each row pile in the group pile for spacing 5D

Pile Arrangement	Lead Row	2nd Row	3rd Row	4th Row	5th Row	6th Row	7th Row	8th Row	9th Row	10th Row
2×2	198.65	179.40								

2×3	198.40	178.65	164.15							
2×4	198.50	178.05	162.90	154.90						
2×5	227.65	163.70	138.90	124.00	117.95					
2×10	207.95	177.30	159.45	149.45	143.55	141.85	141.10	141.65	144.25	148.20
3×2	187.60	166.93								
3×3	189.53	164.53	148.53							
3×4	188.47	162.10	143.00	136.20						
3×5	187.33	160.80	141.67	131.67	131.03					
3×10	200.90	163.53	142.03	130.77	123.97	123.97	120.30	117.90	120.70	127.30
4×2	182.03	159.93								
4×3	180.00	153.60	137.88							
4×4	183.05	154.23	132.65	125.00						
4×5	181.75	152.23	131.08	119.78	119.40					
4×10	198.38	156.73	132.33	118.28	110.57	107.40	106.14	105.73	108.34	116.58
5×2	178.32	155.76								
5×3	175.70	147.88	131.42							

5×4	179.58	148.02	119.06	117.48						
5×5	178.18	147.02	124.40	112.10	111.35					
5×10	195.02	152.50	127.82	113.77	105.42	101.73	100.20	99.12	100.78	107.99
10×2	163.56	140.28								
10×3	144.72	133.39	114.43							
10×4	135.10	129.21	105.37	96.66						
10×5	170.83	119.72	108.16	91.00	88.15					
10×10	180.16	142.41	114.07	98.00	88.63	83.96	81.51	79.79	80.09	86.05

Table 4.3: Average shear force for each row pile in the group pile for spacing 7D

Pile Arrangement	Lead Row	2nd Row	3rd Row	4th Row	5th Row	6th Row	7th Row	8th Row	9th Row	10th Row
2×2	217.60	197.55								
2×3	216.50	199.70	181.95							
2×4	218.75	199.00	185.10	175.70						
2×5	203.70	207.40	191.15	183.80	176.15					
2×10	219.75	186.05	167.05	157.45	153.35	152.20	153.45	156.20	161.05	176.00

3×2	210.40	187.67								
3×3	214.27	189.97	169.10							
3×4	213.70	187.50	168.67	158.57						
3×5	228.93	194.77	172.87	163.30	157.43					
3×10	215.43	173.77	149.40	136.90	132.30	132.30	131.47	134.40	139.37	157.07
4×2	207.43	182.65								
4×3	206.25	179.70	159.63							
4×4	211.35	181.53	159.68	149.18						
4×5	228.78	190.00	165.25	154.15	148.48					
4×10	211.93	167.78	141.73	128.33	122.93	121.35	122.05	125.10	129.58	148.25
5×2	204.60	177.54								
5×3	203.16	173.72	152.36							
5×4	209.58	176.10	151.74	140.22						
5×5	228.66	185.88	158.88	145.26	138.60					
5×10	209.90	163.94	136.50	122.64	117.34	116.04	117.02	119.34	124.04	142.02
10×2	182.38	161.88								

10×3	179.67	146.19	134.47							
10×4	178.30	142.31	117.73	121.83						
10×5	179.48	144.51	120.46	108.56	116.54					
10×10	204.01	153.26	123.30	107.18	100.11	97.93	99.21	101.95	108.40	140.14

Graphical representation of Lateral Force vs Rows

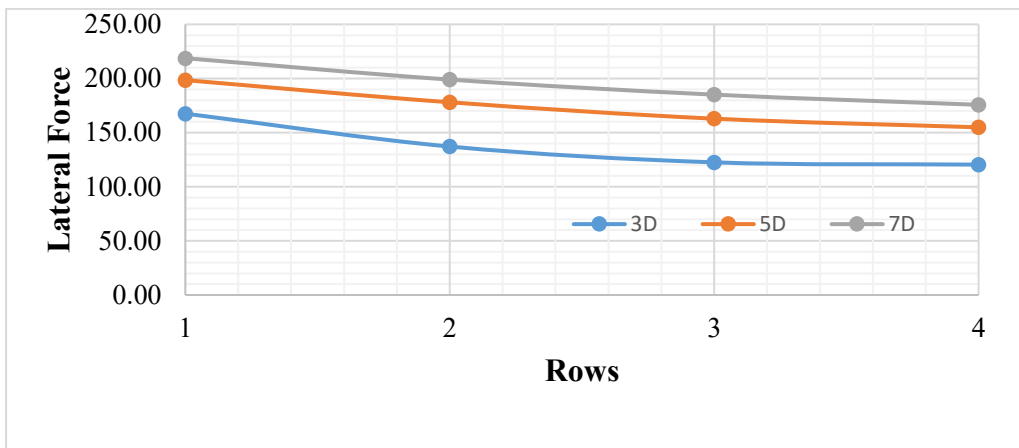


Figure 4.14: Variation of lateral force with row position for 2x4.

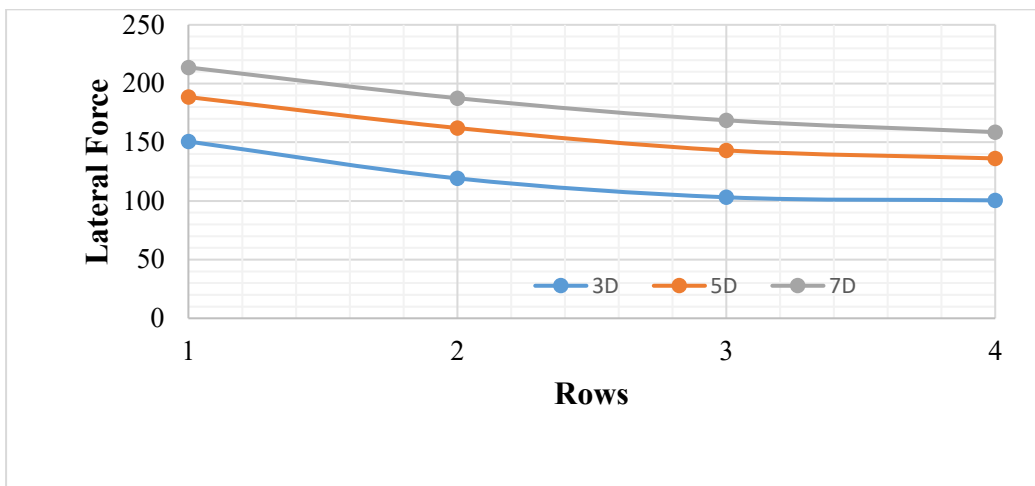


Figure 4.15: Variation of lateral force with row position for 3x4.

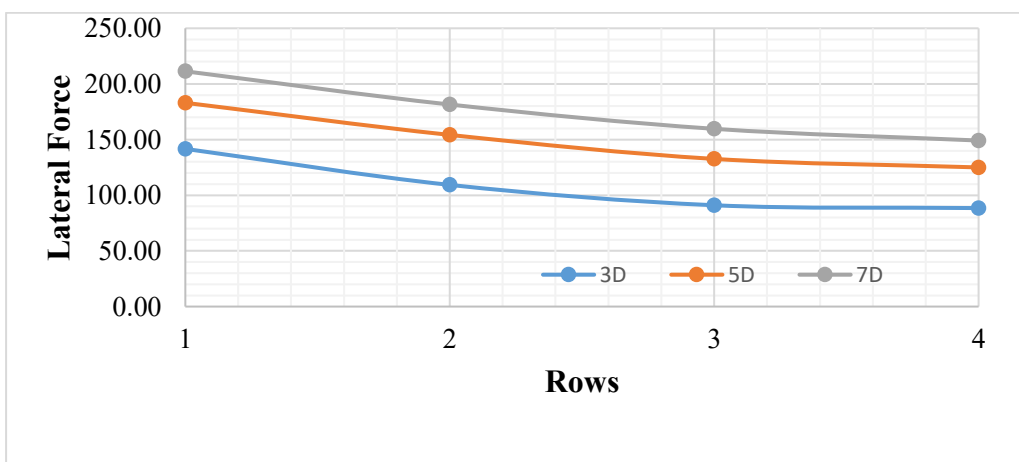


Figure 4.16: Variation of lateral force with row position for 4x4.

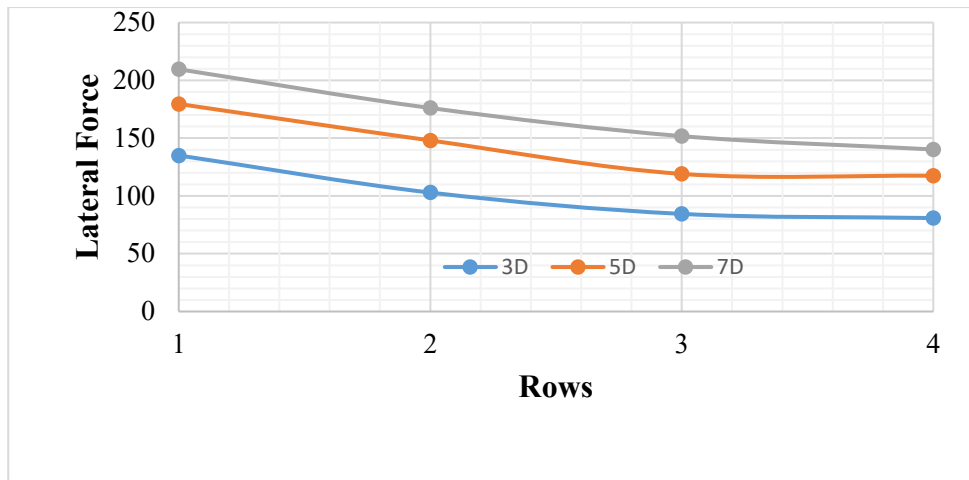


Figure 4.17: Variation of lateral force with row position for 5×4.

The above analysis of lateral force for spacing, it indicates that with an increase in spacing, lateral force increases, and also the lateral force decreases from the lead row to the middle row and trailing row. The results show that lateral resistance decreases as the number of rows increases from one to four for all spacing from 3D to 7D. This reduction in lateral resistance with increasing number of rows is mainly attributed to overlapping stress zones within the surrounding soil mass, which decreases the efficiency of individual piles in resisting lateral loads.

From an engineering design standpoint, our results show that increasing the spacing can give additional safety margins against lateral loading, particularly for bridge foundation systems subjected to substantial horizontal forces such as wind, seismic action, and traffic-induced loads. The efficiency of individual piles decreases with increasing pile row number due to group interaction effects, but the overall stability of the pile group can still be increased by increasing spacing. 7D spacing can therefore be considered to be more successful in achieving stronger lateral resistance and providing safer pile foundation performance under lateral stress situations.

4.3.4 Evaluation of p -multiplier for group pile

The p - y Curve is modified by p -multipliers to account for shadowing effects within pile groups (Abdrabbo & Gaaver, 2012). The p -multipliers generally decrease with decreasing S/D and increasing soil stiffness, and fixed-head conditions result in lower multipliers due to enhanced group interaction effects. (Adeel et.al 2020). The below p -multiplier factors show that there is an increase in the value of p -multiplier from the lead row to the 10th row, and all the p -multipliers satisfy the range of value of p -multiplier given by (Brown et al., 1988) and (Abdrabbo & Gaaver, 2012). At smaller pile spacing, the stress zones generated around

individual piles overlap significantly, which reduces the effective soil resistance available to each pile. This behavior is commonly known as the shadowing effect, where trailing piles experience reduced soil resistance due to disturbance caused by leading piles. As the pile spacing increases, the overlapping of the influence zones reduces, and each pile mobilizes more independent lateral resistance from the surrounding soil, and the p-multiplier increases (Jones et al., 2022).

Table 4.4: *p*-multiplier factor for each row pile in the group pile for 3D

Pile Arrangement	Lead Row	2nd Row	3rd Row	4th Row	5th Row	6th Row	7th Row	8th Row	9 th Row	10 th Row
2×2	0.76	0.63								
2×3	0.76	0.63	0.59							
2×4	0.77	0.63	0.56	0.55						
2×5	0.77	0.63	0.57	0.52	0.53					
2×10	0.79	0.64	0.57	0.53	0.50	0.49	0.48	0.47	0.46	0.49
3×2	0.68	0.57								
3×3	0.69	0.55	0.51							
3×4	0.69	0.55	0.47	0.46						
3×5	0.70	0.55	0.48	0.43	0.43					
3×10	0.72	0.56	0.48	0.43	0.41	0.41	0.39	0.37	0.38	0.43
4×2	0.64	0.53								
4×3	0.64	0.50	0.46							
4×4	0.65	0.50	0.42	0.41						

4×5	0.66	0.51	0.43	0.37	0.38					
4×10	0.68	0.52	0.44	0.39	0.36	0.34	0.33	0.31	0.30	0.33
5×2	0.62	0.51								
5×3	0.61	0.47	0.42							
5×4	0.62	0.47	0.39	0.37						
5×5	0.63	0.48	0.39	0.34	0.34					
5×10	0.74	0.53	0.43	0.38	0.34	0.32	0.31	0.30	0.28	0.32
10×2	0.56	0.45								
10×3	0.55	0.41	0.36							
10×4	0.58	0.42	0.32	0.29						
10×5	0.61	0.43	0.33	0.26	0.26					
10×10	0.62	0.45	0.36	0.30	0.26	0.24	0.22	0.19	0.17	0.21

Table 4.5: *p*-multiplier factor for each row pile in the group pile for 5D

Pile Arrangement	Lead Row	2nd Row	3rd Row	4th Row	5th Row	6th Row	7th Row	8th Row	9 th Row	10 th Row
2×2	0.91	0.82								
2×3	0.91	0.82	0.75							

2×4	0.91	0.82	0.75	0.71						
2×5	1.04	0.75	0.64	0.57	0.54					
2×10	0.95	0.81	0.73	0.69	0.66	0.65	0.65	0.65	0.66	0.68
3×2	0.86	0.77								
3×3	0.87	0.76	0.68							
3×4	0.86	0.74	0.66	0.63						
3×5	0.86	0.74	0.65	0.60	0.60					
3×10	0.92	0.75	0.65	0.60	0.57	0.57	0.55	0.54	0.55	0.58
4×2	0.84	0.73								
4×3	0.83	0.70	0.63							
4×4	0.84	0.71	0.61	0.57						
4×5	0.83	0.70	0.60	0.55	0.55					
4×10	0.91	0.72	0.61	0.54	0.51	0.49	0.49	0.49	0.50	0.53
5×2	0.82	0.71								
5×3	0.81	0.68	0.60							
5×4	0.82	0.68	0.55	0.54						

5×5	0.82	0.67	0.57	0.51	0.51					
5×10	0.89	0.70	0.59	0.52	0.48	0.47	0.46	0.45	0.46	0.50
10×2	0.75	0.64								
10×3	0.66	0.61	0.53							
10×4	0.62	0.59	0.48	0.44						
10×5	0.78	0.55	0.50	0.42	0.40					
10×10	0.83	0.65	0.52	0.45	0.41	0.39	0.37	0.37	0.37	0.39

Table 4.6: *p*-multiplier factor for each row pile in the group pile for 7D

Pile Arrangement	Lead Row	2nd Row	3rd Row	4th Row	5th Row	6th Row	7th Row	8th Row	9 th Row	10 th Row
2×2	0.999	0.91								
2×3	0.99	0.92	0.84							
2×4	1.00	0.91	0.85	0.81						
2×5	0.93	0.95	0.88	0.84	0.81					
2×10	1.01	0.85	0.77	0.72	0.70	0.70	0.70	0.72	0.74	0.81
3×2	0.97	0.86								

3×3	0.98	0.87	0.78							
3×4	0.98	0.86	0.77	0.73						
3×5	1.05	0.89	0.79	0.75	0.72					
3×10	0.99	0.80	0.69	0.63	0.61	0.61	0.60	0.62	0.64	0.72
4×2	0.95	0.84								
4×3	0.95	0.82	0.73							
4×4	0.97	0.83	0.73	0.68						
4×5	1.05	0.87	0.76	0.71	0.68					
4×10	0.97	0.77	0.65	0.59	0.56	0.56	0.56	0.57	0.59	0.68
5×2	0.94	0.81								
5×3	0.93	0.80	0.70							
5×4	0.96	0.81	0.70	0.64						
5×5	1.05	0.85	0.73	0.67	0.64					
5×10	0.96	0.75	0.63	0.56	0.54	0.53	0.54	0.55	0.57	0.65
10×2	0.84	0.74								
10×3	0.82	0.67	0.62							

10×4	0.82	0.65	0.54	0.56						
10×5	0.82	0.66	0.55	0.50	0.53					
10×10	0.94	0.70	0.57	0.49	0.46	0.45	0.46	0.47	0.50	0.64

4.3.5 Effect of pile spacing on p-multiplier

The relationship between the p-multiplier and spacing ratio shows that wider spacing between piles improves the lateral load resistance of pile groups. When the spacing is limited to 3D, intense interaction among piles and the surrounding soil restricts the development of soil resistance, which leads to lower p-multiplier values. As spacing extends to 5D and 7D, interaction effects decrease significantly, and the behavior of piles resembles that of isolated single piles as pile interaction becomes negligible at larger spacing (IRC:78,2014).

Generally, the p-multiplier values of the leading row piles are higher than the trailing rows due to the undisturbed soil in the loading direction (Brown et al., 1988). However, the difference between the first and last row multipliers decreases with higher spacing, indicating a better load-sharing efficiency within the pile group.

These findings validate that an increased spacing ratio improves lateral resistance capability and reduces shadowing effects between neighboring piles.

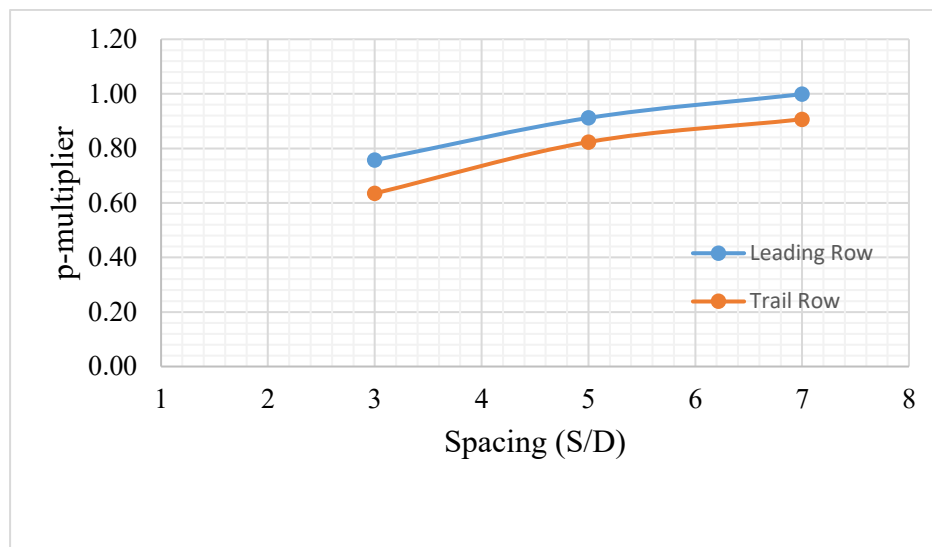


Figure 4.18: Variation of p-multiplier vs spacing (s/d) for pile arrangement 2x2.

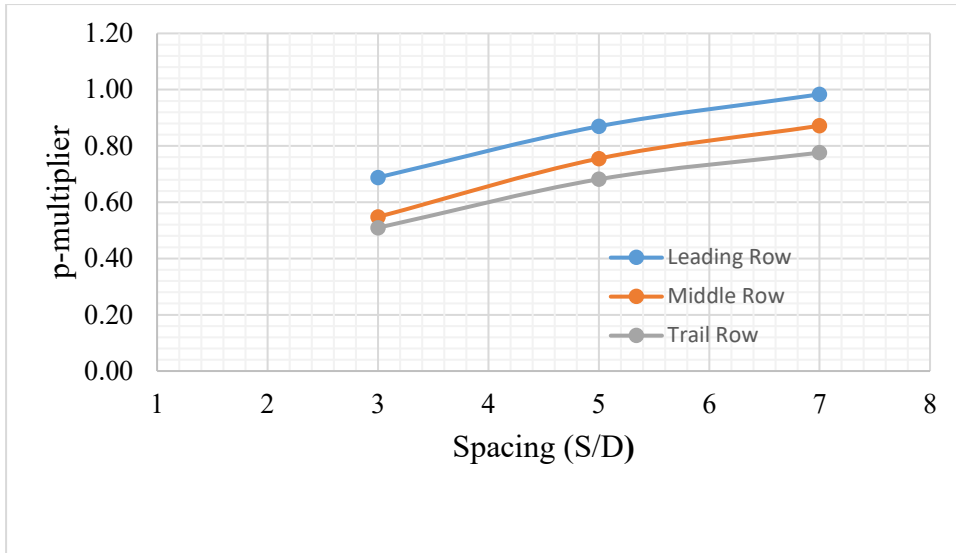


Figure 4.19: Variation of p-multiplier vs spacing (s/d) for pile arrangement 3×3.

The results show that pile spacing significantly affects lateral behavior. At 3D spacing, strong pile interaction increases displacement and reduces capacity, while at 7D spacing, interaction becomes minimal and the pile group behaves nearly like single piles. Therefore, increasing spacing improves lateral resistance and reduces deflection.

5 CONCLUSIONS AND RECOMMENDATIONS

5.1 Conclusions

From the above analysis of Finite Element Analysis using the Bowles (1997) for modulus of elasticity, using interface strength 0.67, and for fine mesh size for lateral displacement of 1% of the diameter according to IRC:78 2014, the following findings are summarized below:

- The increase in diameter from 0.8m-2.0m there is increase in lateral load capacity. With an increase in diameter from 11%-25%, there is an increase in lateral load capacity from 32%-72%.
- The research indicates that the critical depth affecting the lateral resistance is around 15D, where D is the diameter of the pile. This indicates that the embedment beyond this depth does not substantially improve lateral capacity; thus, pile design for lateral loading may be maximized by using 15 D as the effective depth for resistance under the examined soil conditions.
- The lateral load capacity and its variation trend are strongly affected by changes in the groundwater level. An increase in the water table tends to reduce lateral displacement. In this study, the water level was varied from +8 m to -8 m. The results indicate that when the water level rises above the ground surface, it does not significantly influence the lateral load capacity.
- From Plaxis-3D analysis in group pile, the magnitude of shear force and p-multiplier carried by the lead row is greater than preceding rows, and it satisfies the concept of previous research done on the basis of field value and laboratory experiment.
- The Pile behaves as an isolated single pile as spacing increases to 7D, as pile interaction becomes negligible at larger spacing.

Most of the international studies have considered uniform soil conditions for lateral pile resistance. The lateral stiffness of piles is dependent on soil-pile interaction, which is affected by the varying soil profiles in Nepal (soft clay, sandy deposits, and weathered rock). Bridge foundations in Nepal should consider seismic loading, river scour, and slope instability, unlike cases that only consider traffic and wind loads. Hence, international findings require site-specific modifications for their reliable application in Nepal.

The study provides practical recommendations on pile spacing, critical depth estimation for lateral resistance, and the use of calibrated modeling for the prediction of pile group behavior, which can improve foundation safety and reduce design uncertainties.

5.2 Recommendations

The possible further study may be as follows:

- The soil parameters can be varied for further study.
- Validation can be done by the lateral load analysis of the pile test.
- Other advanced models can be used and compared for better results.
- The simplified design methods and codes can be used to compare results.

Future research should include the effects of cyclic lateral loading, layered riverbed soil conditions, full-scale lateral pile load testing, and seismic response of pile groups. These studies would help in improving the prediction accuracy and assist in the development of Nepal-specific bridge foundation design guidelines.

The study shows that the pile foundations are adequate to bear the applied lateral loads within allowable displacement limits, with most of the lateral soil resistance mobilized by the adequate embedment depth. The pile spacing was satisfactory, although the interaction effects on the pile group were observed. In the future design of bridge foundations, lateral load analysis, optimized pile spacing, and three-dimensional numerical modeling should be adopted to improve prediction accuracy and structural reliability.

The findings of this study suggest that the Department of Roads, Nepal to incorporate the guidelines for the assessment of lateral pile behavior in bridge foundation design. Mandatory lateral pile load testing may not be economically feasible, but it should be encouraged for major structures in sandy riverbed deposits and high seismic risk areas. For routine projects, validated three-dimensional numerical modeling can reliably predict lateral pile response.

6 REFERENCES

- Abbas Al-Shamary, J. M., Chik, Z., & Taha, M. R. (2018). Modeling the lateral response of pile groups in cohesionless and cohesive soils. *International Journal of Geo-Engineering*, 9(1), 1.
- Abdrabbo, F. M., & Gaaver, K. E. (2012). Simplified analysis of laterally loaded pile groups. *Alexandria Engineering Journal*, 51(2), 121–127.
- Bathe, K. J. (1996). *Finite Element Procedures*. Prentice Hall.
- Bouafia, A. (2023). New p–y curve formulation for laterally loaded single piles based on pressuremeter tests. *Arabian Journal of Geosciences*, 16, 684.
- Bowles, J. E., & Guo, Y. (1996). *Foundation analysis and design* (Vol. 5). McGraw-hill.
- Brinkgreve, R. B. J. (2021). *PLAXIS CONNECT Edition V21.01 Material Models Manual*.
- Broms, B. B. (1964). Lateral resistance of piles in cohesionless soils. *Journal of the Soil Mechanics and Foundations Division*, 90(3), 123–156.
- Brown, D. A., Morrison, C., & Reese, L. C. (1988). Lateral load behavior of pile group in sand. *Journal of Geotechnical Engineering*, 114(11), 1261–1276.
- Chandrasekaran, S. S., Boominathan, A., & Dodagoudar, G. R. (2010). Group interaction effects on laterally loaded piles in clay. *Journal of Geotechnical and Geoenvironmental Engineering*, 136(4), 573–582.
- Congress, I. R. (n.d.). *Standard Specifications and Code of Practice for Road Bridges*. VII.
- Cook, R. D., Malkus, D. S., Plesha, M. E., & Witt, R. J. (2001). *Concepts and Applications of Finite Element Analysis* (4th ed.). Wiley.
- David V. Griffiths, D. V., & Paul A. Lane, P. A. (1999). Slope Stability Analysis by Finite Elements. . *Géotechnique*.
- Degago, S. A., Jostad, H. P., Olsson, M., Grimstad, G., & Nordal, S. (2010). Time- and stress-compressibility of clays during primary consolidation. *Numerical Methods in Geotechnical Engineering - Proceedings of the 7th European*

- Conference on Numerical Methods in Geotechnical Engineering*, 125–130.
<https://doi.org/10.1201/b10551-25>
- Derrick, N. (2020). Effect of Mesh Size on Soil-Structure Interaction in Finite Element Analysis. *International Journal of Engineering Research And*, 9(06), 802–807. <https://doi.org/10.17577/ijertv9is060655>
- Duncan, J. M., & Wright, S. G. (2005). *Soil Strength and Slope Stability*. John Wiley & Sons.
- El Gendy, M. (2025). Analyzing laterally loaded piles in multi-layered cohesive soils: a hybrid beam on nonlinear Winkler foundation approach with case studies and parametric study. *Discover Civil Engineering*, 2(1), 77.
- Elhakim, A. F., El Khouly, M. A. A., & Awad, R. (2016). Three dimensional modeling of laterally loaded pile groups resting in sand. *HBRC Journal*, 12(1), 78–87.
- (FHWA), F. H. A. (1996). Design and Construction of Driven Pile Foundation, Publication No. *FHWA-HI-97-13*.
- Garcia, J. R., & De Albuquerque, P. J. R. (2018). 3D numerical modeling applied to analysis of piled foundations. *Ingeniare*, 26(4), 663–672.
<https://doi.org/10.4067/S0718-33052018000400663>
- GEER Association. (2015). *Geotechnical Engineering Reconnaissance of the 2015 Gorkha Nepal Earthquake*.
- Gupta, S. K., & Dahal, B. K. (2023a). Finite Element Analysis on Load-Settlement Behavior of Axially Loaded Pile on Sand. *Journal of Engineering Technology and Planning*, 4(1), 72–81. <https://doi.org/10.3126/joetp.v4i1.58443>
- Gupta, S. K., & Dahal, B. K. (2023b). Finite Element Analysis on Load-Settlement Behavior of Axially Loaded Pile on Sand. *Journal of Engineering Technology and Planning*, 4(1), 72–81. <https://doi.org/10.3126/joetp.v4i1.58443>
- Hashash, Y. M. A. , et al. (2015). *Geotechnical field reconnaissance of the 2015 Nepal earthquakes*.

- Ilyas, T., Leung, C. F., Chow, Y. K., & Budi, S. S. (2004). Centrifuge model study of laterally loaded pile groups in clay. *Journal of Geotechnical and Geoenvironmental Engineering*, 130(3), 274–283.
- Institute, A. P. (1977). *Division of Production*. API Recommended Practice for Planning.
- IS 2911 (Part 4). (1985). *Code of Practice for Design and Construction of Pile Foundations – Load Test on Piles*.
- Isenhower, W. M., Shin-Tower, P. E., & Wang, P. E. (n.d.). *User's Manual for LPile 2016 (Using Data Format)*.
- Jones, K., Sun, M., & Lin, C. (2022). Numerical analysis of group effects of a large pile group under lateral loading. *Computers and Geotechnics*, 144, 104660.
- Kavitha, P. E., Beena, K. S., & Narayanan, K. P. (2016). A review on soil–structure interaction analysis of laterally loaded piles. *Innovative Infrastructure Solutions*, 1(1), 14.
- Kendall E. Atkinson. (1989). *An Introduction to Numerical Analysis*. Wiley.
- Kim, Y., & Jeong, S. (2011). Analysis of soil resistance on laterally loaded piles based on 3D soil–pile interaction. *Computers and Geotechnics*, 38(2), 248–257.
- Kulhawy, F. H., & Mayne, P. W. (1990a). Manual on Estimating Soil Properties for Foundation Design. *Ostigov*, 299.
http://www.osti.gov/energycitations/product.biblio.jsp?osti_id=6653074
- Kulhawy, F. H., & Mayne, P. W. (1990b). Manual on Estimating Soil Properties for Foundation Design. *Ostigov*, 299.
http://www.osti.gov/energycitations/product.biblio.jsp?osti_id=6653074
- Lao, Y., Takemura, J., Hsiao, W., & Takahashi, A. (2026). Centrifuge modeling-based py curves for laterally loaded monopiles in sand considering the effect of pile-soil relative stiffness. *Ocean Engineering*, 352, 124518.
- Lee, J., Kyung, D., Hong, J., & Kim, D. (2011). Experimental investigation of laterally loaded piles in sand under multilayered conditions. *Soils and Foundations*, 51(5), 915–927.

- Liu, W., Li, H., Weng, X., Wang, Z., Chen, Q., Lei, Y., others, & Feng, Y. (2025). Numerical study on the effect of pile shape and loading direction on the lateral response of displacement pile in sand. *Scientific Reports*, *15*(1), 26653.
- Liyanapathirana, D. S., Carter, J. P., & Airey, D. W. (2005). Numerical Modeling of Nonhomogeneous Behavior of Structured Soils during Triaxial Tests. *International Journal of Geomechanics*, *5*(1), 10–23. [https://doi.org/10.1061/\(asce\)1532-3641\(2005\)5:1\(10\)](https://doi.org/10.1061/(asce)1532-3641(2005)5:1(10))
- M. Laporte, L Bollinger, Lyon-Caen, & h Hoste-Colomer. (2021). Seismicity in far western Nepal reveals flats and ramps along the Main Himalayan Thrust. *Geophysical Journal International*, *226*(3), 1747-1763.
- Marjanović, M., Vukićević, M., & König, D. (2020). Flexible pile group interaction factors under arbitrary lateral loading in sand. *Journal of Marine Science and Engineering*, *8*(10), 800.
- McVay, M. C., Zhang, L., Han, S., & Lai, P. (2000). Experimental and numerical study of laterally loaded pile groups with pile caps at variable elevations. *Transportation Research Record*, *1736*(1), 12–18.
- McVay, M., Zhang, L., Molnit, T., & Lai, P. (1998). Centrifuge testing of large laterally loaded pile groups in sands. *Journal of Geotechnical and Geoenvironmental Engineering*, *124*(10), 1016–1026.
- MUNI BUDHU. (2010). SOIL MECHANICS AND FOUNDATIONS. In *JOHN WILEY & SONS, INC.* (Vol. 1, Number August).
- Nasasira Derrick. (2020). Effect of Mesh Size on Soil-Structure Interaction in Finite Element Analysis. *International Journal of Engineering Research And*, *V9*(06), 802–807. <https://doi.org/10.17577/ijertv9is060655>
- Potts, D. M., & Zdravković, L. (2001). *Finite element analysis in geotechnical engineering. Application*. Thomas Telford.
- Poulos, H. G., & Davis, E. H. (1980a). *Pile Foundation Analysis and Design*. Wiley.
- Poulos, H. G., & Davis, E. H. (1980b). *Pile foundation analysis and design (No. Monograph)*.
- R. K. Devkota. (2022). Parametric Study on Slope Reinforced With Pile. *B.K Dahal*.

- Reddy, J. N. (2006). *An Introduction to the Finite Element Method* (3rd ed.). McGraw-Hill.
- Reese, C., Wang, T., & Vasquez, L. (2006). *Computer Program GROUP Version 7*. Tech. Manual.
- Reese, L. C., Cox, W. R., & Koop, F. D. (1974, May). Analysis of laterally loaded piles in sand. *Offshore Technology Conference* (Pp. OTC-2080). OTC.
- Rollins, K. M., Peterson, K. T., & Weaver, T. J. (1998). Lateral load behavior of full-scale pile group in clay. *Journal of Geotechnical and Geoenvironmental Engineering*, 124(6), 468–478.
- S. Mukherjee, & A. Dey. (2016). Analysis of laterally loaded fixed headed single floating pile in multilayered soil using BEF approach. *In Proceedings of the National Seminar on Geotechnics for Infrastructure Development, Kolkata* (Pp. 1-12).
- Saran, S., & Kumar, S. (2022). *Routine Pile Load Test : A Case Study of Bagdwar Khola Bridge*. 8914, 1766–1772.
- Sert, S. (2003). *Numerical analysis of settlement of piled foundations*. <https://www.researchgate.net/publication/317560899>
- Shiva Saran Timalisina A. (2022). *Numerical Study on Bored Cast In-Situ Pile in Sandy Soil from Routine Pile Load Teste*. A Thesis Defence Report.
- V Jagota, A. S. K. K. (2013). Finite element method: an overview. *Walailak Journal of Science and Technology (WJST)*, 2013•wjst.Wu.Ac.Th.
- Vesic, A. S. (1977). Design of pile foundations. *NCHRP Synthesis of Highway Practice*, 42.
- Wei, W., Wang, F., Yang, F., & Guo, C. (2024). Influence of soil and pile properties on the critical length of laterally loaded piles. *Applied Ocean Research*, 150, 104091.
- Zeng, F., & Jiang, C. (2025). Cyclic py curve modeling for laterally loaded two-pile group in sand based on the strain wedge model. *Computers and Geotechnics*, 187, 107499.

- Zhang, L., McVay, M. C., & Lai, P. (1999). Centrifuge modelling of laterally loaded single battered piles in sands. *Canadian Geotechnical Journal*, 36(6), 1074–1084.
- Zhou, Y., & Tokimatsu, K. (2018). Numerical Evaluation of Pile Group Effect of a Composite Group. *Soils Found.*, 58, 1059–1067.
- Zienkiewicz, O. C., Taylor, R. L., & Zhu, J. Z. (2005). *The Finite Element Method: Its Basis and Fundamentals*. Elsevier.

Annex-I Paper Publication



Numerical Analysis of Laterally Loaded Pile in Sandy Soil

Pooja Singh ^{a,b}, Bhim Kumar Dahal ^c

^{a,d} Department of Civil Engineering, Institute of Engineering, Pulchowk Campus, Tribhuvan University, Kathmandu, Nepal

^c Water Resources Research and Development Centre, Ministry of Energy, Water Resources and Irrigation, Government of Nepal

✉ ^{a,b} 079msgte013.pooja@pcampus.edu.np, ^d bhimd@pcampus.edu.np

Abstract

Piles subjected to lateral forces are commonly used to support structures exposed to horizontal actions such as wind, waves, and seismic loading. Reliable estimation of their lateral performance in sandy soils is crucial for ensuring both the safety and economic consequences. This study numerically examines a single pile under lateral loading using PLAXIS 3D, where the Mohr–Coulomb constitutive model is adopted to represent the nonlinear behavior of sandy soil. The numerical model is analyzed using different soil-pile interaction and different value of modulus of elasticity and the settlement results are compared with the field settlement value to validate the numerical model. The modulus of elasticity proposed by Bowles (1997) and interface strength 67% are determined to be the closest to field data value. The validated model is used to analyze the lateral load behaviour, deflection patterns for different diameter and length, soil–pile interaction characteristics, mesh analysis and ultimate lateral load capacity of pile.

Keywords

Constitutive Model; Lateral Load Capacity; Numerical Analysis; Sandy Soil

1. Introduction

Piles are not only subject to vertical loads but also to significant lateral loads, which arise from wind, earthquakes, wave forces or earth pressures. The lateral load capacity of a pile is a critical parameter that quantifies how much horizontal force the pile can sustain before excessive deflection or failure, and it is typically evaluated using the non-linear p–y curve method, which models the soil–pile interaction as a series of springs where resistance (p) depends on local deflection (y) and soil stiffness. [1]

With the advancement of computational tools, the finite element method (FEM) has become a powerful approach to simulate the behavior of laterally loaded piles. PLAXIS 3D, a widely used FEM-based geotechnical software, enables detailed analysis of pile foundations by representing the pile as a volume or embedded beam element within a 3D soil continuum. The program allows for the use of advanced constitutive soil models, such as the Mohr–Coulomb or Hardening Soil models, which can represent the nonlinear and stress-dependent behavior of sandy soils with high accuracy. [2] Linearly elastic perfectly plastic Mohr column the simplest model involves the cohesion (c), friction angle (ϕ), dilation angle (ψ), Young's modulus (E), and Poisson's ratio (ν). [2] The numerical analysis using the Mohr Column constitutive model provides satisfactory prediction for pile settlement within the sandy layer. [3] The careful selection of soil constitutive models and their associated parameters is pivotal for achieving reliable predictions for employing the Finite Element Method (FEM). [4] The study investigate the parametric analysis of laterally loaded sandy soil by numerical analysis method and the model is validated by using the pile load test data from the site.

There has been conducted many research to analyze the characteristics of sand and clay. [5] Mohr column constitutive

model with soil parameters cohesion (c), friction angle (ϕ), dilation angle (ψ), Young's modulus (E), and Poisson's ratio (ν) for sandy soil is analysed for this research. [2] This literature presents a wide spectrum of values for E adapted from FHWA-IF-020-034 [Web (1969), Chaplin (1963), Papadopoulos (1982), Bowles (1996), Kulhawy and Mayne (1990) for sand (Jones,2020), leading to noteworthy disparities. The value of poisons ratio is narrower than E, so less emphasis is typically placed on precise determination of Poisson's ratio. [6]

Finite element modelling has become a primary tool for analyzing soil–structure interaction in laterally loaded piles as it captures nonlinear soil behaviour more effectively than traditional analytical methods. [7] Early studies using linear elastic–perfectly plastic constitutive laws such as the Mohr–Coulomb model demonstrated limited ability to represent confining-stress effects and dilatancy in sands. [8] Subsequent research showed that simplified constitutive models often underestimate pile head deflection and bending moments under lateral loading conditions. [9] Numerical studies confirm that applying calibrated stiffness parameters and realistic interface conditions significantly improves agreement with experimental load–displacement responses. [10]

Comparative studies show that validated FEM models can accurately represent lateral resistance mechanisms across a range of soil densities and pile geometries. [9] Overall, the literature consistently recognizes FEM as a robust and reliable framework for evaluating the lateral performance of piles in sandy soils when properly calibrated and validated. [10]

1.1 Site Description

The bridge project is located across the Mahuli River in the Saptari region of Province 2 (Ch. 160+700). Along Nepal's East-West Highway, there are a large number of rivers flowing from north to south. The site has a flat topography. The

project's location is in Nepal's eastern Terai region. It is the northern extension of the Indo-Gangetic Plain, 100 to 200 m above sea level, with a subtropical climate. It stretches northward from the foot of the Siwalik Hills to the Nepal-India border in the south, varying between 10 and 50 kilometers in width. There are three further Terai regions: the northern (Bhabar), central, and southern zones. In the north, close to the foot of the mountains, the Terai Zone consists of coarse gravels, which gradually become finer in the south. The approximate coordinates of the site are 26.644797° E and 86.816281° N (Engineering, 2021), as shown in Figure 1.



Figure 1: Google map of site Location

2. Methodology

The methodology for the study involves a structured sequence of procedures beginning with the selection of geotechnical parameters based on laboratory and published data, followed by the development of a three-dimensional numerical model representing the pile, soil domain, and boundary conditions. The model is discretized using an appropriate mesh density to ensure numerical stability and accuracy. It includes several steps geometry, soil exploration and properties, numerical analysis, validating model by pile load test.

2.1 Geometry

The pile is modelled as volume element which gives very realistic interaction with the soil.[11] The finer mesh is used around the pile shaft ensures that lateral deflection, are captured with high accuracy.[11] The mesh size employed was asymmetric comprising 10 node triangular element enabling calculation for the actual model size. The dimension of the model was taken as 20×20×30 which is actually the 20 B on x and y plane and (9+10B) along z axis.

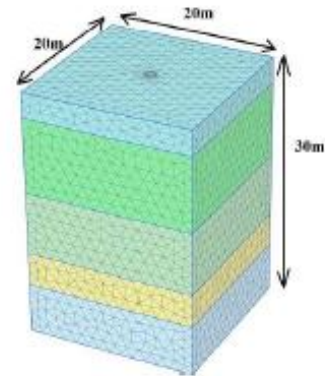


Figure 2: Geometry

2.2 Soil Exploration and Properties

The type of exploration used at the site is standard penetration test according to the site condition. Most parameters were determined through laboratory and field investigations, with some relying on correlations (Kulhawy Mayne, 1990b). Standard penetration test (SPT) results are recorded at varying depths and are shown starting with Table 1.

Layer	SPT Value)	Unit weight unsat (kN/m ³)	Effective Young Modulus (Mpa) Bowles (1997)	Effective Poisson's Ratio	Effective Friction Angel (degree)
Layer1	16	18	24220	0.28	30
Layer2	24	18	33541	0.27	30
Layer3	32	18	40927	0.29	31
Layer4	30	18	34756	0.28	32
Layer5	47	18	47940	0.30	32

Table 1: Soil Properties

Layer	Tromie nkov (1974) Mpa	WEB (1969) Mpa	Chaplin (1963) Mpa	Papado poulous (1982) Mpa	Kulhawy and Mayne (1990)) Mpa
Layer1	42114	16620	14650	20300	11000
Layer2	48121	20824	19790	26565	21166
Layer3	53627	26383	25860	34560	31400
Layer4	48647	21270	20260	27230	22666
Layer5	58523	33247	32885	45100	43000

Table 2: Modulus of Elasticity (Mpa)

Materials	Concrete
Length (m)	22.77
Outer Diameter (m)	1
Young's Modulus (GPa)	29.58
Poisson's ratio	0.15

Table 3: Pile Properties

2.3 Pile Properties

Piles are deep foundation elements that transfer structural loads to competent soil or rock strata when surface soils are inadequate.[12] A pile load test is a field-based verification method used to assess the actual load-displacement behaviour of a pile under controlled loading.[13] Static pile load tests, including compression, tension, and lateral tests, directly determine the ultimate load capacity and serviceability performance of the pile.[14] The characteristics and dimension of pile are in Table 2.

2.4 Pile Load Test

The pile load test is conducted to evaluate the load-settlement response and ultimate compressive capacity of a cast-in-situ pile under controlled static loading conditions, typically following procedures outlined in international standards such as ASTM D1143 .[15] This method fundamentally assesses the mobilization of side friction and end-bearing resistance by interpreting the nonlinear load-settlement relationship, enabling engineers to distinguish between elastic shortening, soil-pile interface behavior, and tip resistance development.[12] Moreover, this analysis aids in predicting the load settlement behaviour within a single pile using numerical simulation.[16]

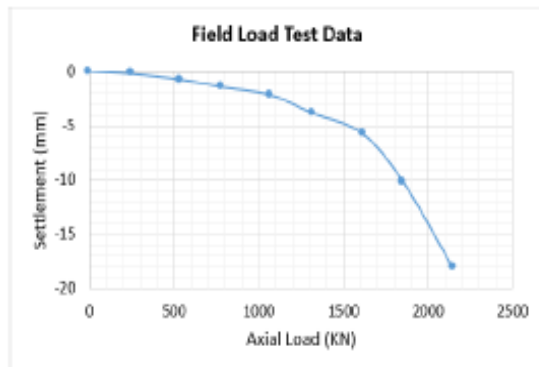


Figure 3: Field Load Test Data

2.5 Numerical Analysis

Numerical Analysis is the method for examining the algorithm for solving mathematical problems employing the numerical approximation. This study employs the Plaxis-3D for modelling and analysis using Mohr column constitutive model for drainage condition being drained as the soil is notable highly permeable. The pile being modelled as linear elastic material. The details for Plaxis-3D model is from PLAXIS CONNECT EDITION V21.01 Material Model

Manual. [2] The fine mesh size is used for analysis as it reduces numerical discretization error. [17]

3. Results and Discussion

3.1 Model Validation

The model is validated using soil pile interaction for different interface strength from 0.5 to 1.0 and different correlation of modulus of elasticity from Bowles (1997), Web (1969), Chaplin (1963), Papadopoulos (1982), Kulhawy and Mayne (1990) and Tromienkov (1974) for sand. The results are compared with the field load test data for vertically loaded pile of diameter 1.0 and length 22.77m. The results shows that interface strength 0.67 and Bowles (1997) gives close prediction to field data.

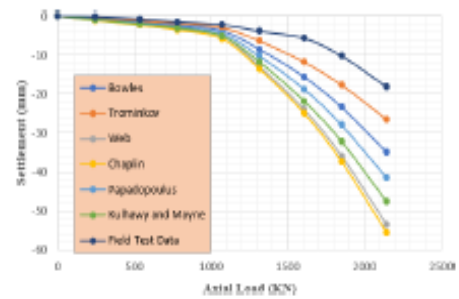


Figure 4: Load vs Settlement for Rinter=0.5

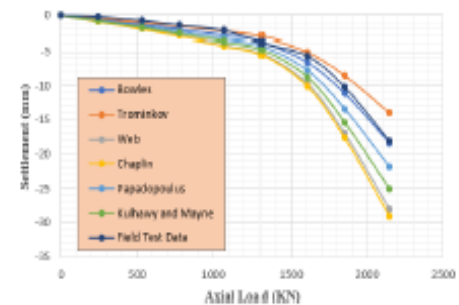


Figure 5: Load vs Settlement for Rinter=0.67

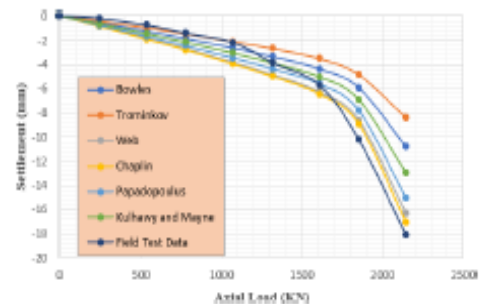


Figure 6: Load vs Settlement for Rinter=0.8

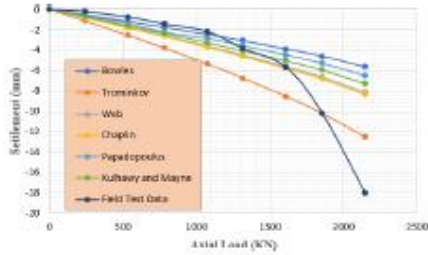


Figure 7: Load vs Settlement for Rinter=1.0

3.2 Lateral Load Analysis

The validated numerical model is used for analysis of behaviour of single laterally loaded pile with different interface strength, different mesh analysis, different diameter and different length. The result accuracy is increased and errors are decreased by incorporating the mesh refinement in the analysis. [18]Plaxis software is a valuable finite element analysis tool.

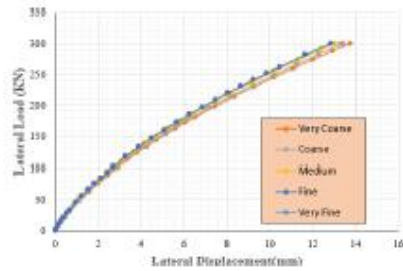


Figure 8: Lateral Load vs Displacement for different Mesh Analysis

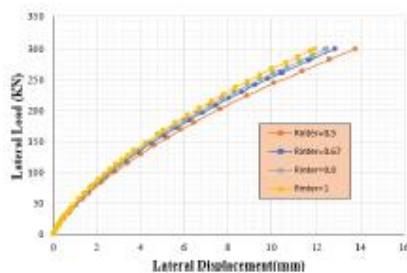


Figure 9: Lateral Load vs Displacement for different interface strength

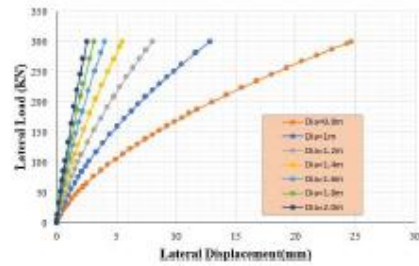


Figure 10: Lateral Load vs Displacement for different diameter of Pile

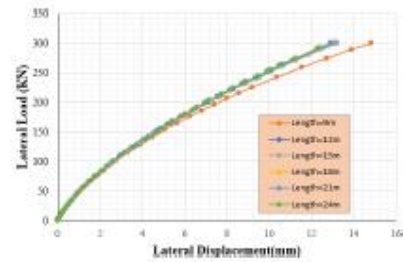


Figure 11: Lateral Load vs Displacement for different length of Pile

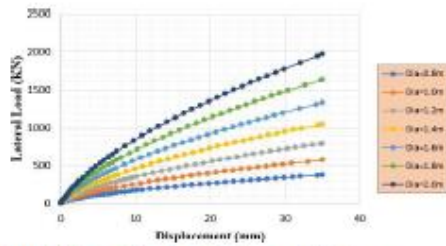


Figure 12: Lateral Load vs Displacement for 35mm Displacement

4. Conclusion

- The finer mesh size produces more accurate result. The interface strength 67% and Bowles (1997) Modulus of elasticity demonstrates close prediction with field settlement value.
- The load-displacement curve for interface Rinter (0.5-1.0) shows there is decrease in lateral displacement value with increase in interface strength.
- The increase in diameter from 0.8m-2.0m there is decrease in lateral displacement from 21% to 63%. For the displacement value of 35mm for diameter (0.8m-2.0m) there is increase in lateral load from 18% to 42%.

- With constant lateral load and increase in length of pile there is minimal variation in lateral displacement.
- The load-displacement curve can be used in the analysis of pile behavior using numerical modeling and the pile bearing capacity can be computed.

- [17] O. C. Zienkiewicz and R. L. Taylor, *The finite element method set*. Elsevier, 2005.
- [18] N. Derrick and A. K. Srivastava, "Effect of mesh size on soil-structure interaction in finite element analysis," *Int J Eng Res Technol*, vol. 96, pp. 802–7, 2020.

References

- [1] K. Yin, L. Li, and E. Di Filippo, "A numerical investigation to determine the p-y curves of laterally loaded piles," *Mathematics*, vol. 9, no. 21, p. 2783, 2021.
- [2] R. Brinkgreve and P. Vermeer, "Plaxis connect edition v22.02 material models manual," *Delft, The Netherlands*, 2021.
- [3] S. K. Gupta and B. K. Dahal, "Finite element analysis on load-settlement behavior of axially loaded pile on sand," *Journal of Engineering Technology and Planning*, vol. 4, no. 1, pp. 72–81, 2023.
- [4] B. K. Dahal, J.-J. Zheng, and R.-J. Zhang, "Evaluation and modelling of the reconstituted clays considering pre-peak stiffness degradation," *International Journal of Geosynthetics and Ground Engineering*, vol. 5, no. 2, p. 9, 2019.
- [5] B. K. Dahal, J. J. Zheng, and R. J. Zhang, "Experimental investigation on physical and mechanical behavior of kathmandu clay," *Advanced Materials Research*, vol. 1145, pp. 112–116, 2018.
- [6] F. H. Kulhawy and P. W. Mayne, "Manual on estimating soil properties for foundation design," Electric Power Research Inst., Palo Alto, CA (USA); Cornell Univ., Ithaca . . . , Tech. Rep., 1990.
- [7] H. Matlock, "Correlation for design of laterally loaded piles in soft clay," in *Offshore technology conference*. OTC, 1970, pp. OTC–1204.
- [8] C. S. Desai and H. J. Siriwardane, "Constitutive laws for engineering materials, with emphasis on geologic materials," (*No Title*), 1984.
- [9] K. M. Rollins, K. T. Peterson, and T. J. Weaver, "Lateral load behavior of full-scale pile group in clay," *Journal of Geotechnical and Geoenvironmental Engineering*, vol. 124, no. 6, pp. 468–478, 1998.
- [10] L. Zhang, Y. Xu, and W. Liu, "Finite element modelling of laterally loaded piles in cohesionless soils," *Soils and Foundations*, vol. 55, no. 5, pp. 1157–1169, 2015.
- [11] S. K. Biswas, S. Mukherjee, S. Chakrabarti, and M. De, "Soil interaction of laterally loaded free head long pile embedded in layered sand medium."
- [12] M. Tomlinson and J. Woodward, *Pile design and construction practice*. CRC press, 2007.
- [13] B. Fellenius, *Basics of foundation design*. Lulu. com, 2017.
- [14] P. Jayasree, K. Arun, R. Oormila, and H. Sreelakshmi, "Lateral load capacity of piles: a comparative study between indian standards and theoretical approach," *Journal of The Institution of Engineers (India): Series A*, vol. 99, no. 3, pp. 587–593, 2018.
- [15] A. International, *Standard test method for deep foundations under static axial compressive load*. ASTM International, 2013.
- [16] L. Zdravkovic', *Finite element analysis in geotechnical engineering: theory*. Thomas Telford, 1999.

Annex-II Soil Exploration




Fig: Hammering 37

Annex-III Static Pile Load Test of Mahuli Bridge

A
FINAL REPORT
ON
STATIC PILE LOAD TEST OF MAHULI BRIDGE
P6-PP3 WORKING PILE



Kathmandu, February 2022

<u>SUBMITTED BY:</u>	<u>SUBMITTED TO:</u>
<p>N.S. ENGINEERING & GEO-TECHNICAL SERVICES PVT. LTD. JAWAGAL, LALITPUR, NEPAL (AN ISO 9001:2015 CERTIFIED COMPANY) TEL: +977-1-5260121 E-MAIL: WE.NSENGINEERING@GMAIL.COM, INFO@NSENGINEERING.COM WEBSITE: WWW.NSENGINEERING.COM.NP</p>	<p>CHINA RAILWAY NO.2 ENGINEERING GROUP CO., LTD.</p> 

1. GENERAL

1.1 Introduction

Static pile load test is an in-situ test to observe the settlement behavior of a pile under an applied load and the most reliable method for determining pile capacities. This test is performed in cast in-situ pile under static axial compressive load testing for Mahuli Bridge P6-PP3 Working Pile.

1.2 Test Purpose

The purpose of the static pile load test is

- To determine the adequacy of pile capacity.
- To determine the load-settlement behavior of a pile, especially in the region of anticipated working load.

1.3 Related Specification

The test load is applied in the increments as specified or approved by the Engineer. These are generally be those recommended in

- Standard Specification of Roads and Bridges
- ASTM D1143_07

2. DETAILS OF TEST PILE

The test pile is cast in-situ piles. The location and test load are decided by the Consultant. The details of test piles are shown in the following table:

Table 1 Details of Test Pile

SN.	Bridge Name	Chainage	Pile ID	Design pile loads (KN)	Date of Casting	Date of Testing
				Pier		
1	Mahuli	K 160+355.012	P6-PP3 Working Pile	1056.83	16 Dec 2021	31 Jan 2022

Additional Information

RL of cutoff (Top) level of pile = 114.562 m

RL of testing level of pile = 117.56 m

3. TEST METHOD

The test was done by application of an axial static load to a single pile by compression method. In this type of test, compression load was applied to the pile top by means of a hydraulic jack acting directly opposite in reaction to the series of statically placed kentledges loads. The loading and unloading process of these weights increments for increasing the loads and decrements for



5. TEST PROCEDURE

5.1 Test preparation

The following preparations were done before commencing the test.

- Excavate or add fill to the ground surface around the test pile to the final design elevation.
- Cut off or build up the test pile as necessary to permit construction of the load-application apparatus, placement of the necessary testing and instrumentation equipment, and observation of the instrumentation.
- Remove any damaged or unsound material from the pile top and prepare the surface so that it is perpendicular to the pile axis with minimal irregularity to provide a good bearing surface for a test plate.
- Install a solid steel test plate at least 25 mm thick perpendicular to the long axis of the test pile that covers the complete pile top area. The test plate is spanned across and between any unbraced flanges on the test pile.

5.2 Loading Procedure

Based on the loading procedures, the load was applied in increment load. Each load increment and decrement were held for a specified interval of time. Readings of gross settlement, load, and time are taken and recorded immediately before and after the application of each load increment and decrement.

Following the application of each load increment and decrement, the load was maintained at the specified value for not less than the time shown on the lower portion of the table or until the rate of settlement is less than 0.25mm/60 min in every stage.

Table 2: Loading and Unloading procedure as per ASTM D 1143/D 1143 M-07

S. N	Designed load (%)	Minimum Holding time	Accumulated Time	Remarks
1	0	0		
2	25	60 minutes		≥ 60 minutes till the settlement rate is ≤ 0.25mm/hour
3	50	60 minutes	1 hour	"
4	75	60 minutes	2 hours	"
5	100	60 minutes	3 hours	"
6	125	60 minutes	4 hours	"
7	150	60 minutes	5 hours	"
8	175	60 minutes	6 hours	"

3

9	200	5 hours	7 hours	till the settlement rate \leq 0.25mm/hour and reaching at least 12 hours from the beginning of test
10	175	60 minutes	12 hours	\geq 60 minutes till the settlement rate is \leq 0.25mm/hour
11	150	60 minutes	13 hours	"
12	125	60 minutes	14 hours	"
13	100	60 minutes	15 hours	"
14	75	60 minutes	16 hours	"
15	50	60 minutes	17 hours	"
16	25	60 minutes	18 hours	"
17	0		19 hours	

5.3 Measurement Procedure

During loading and unloading, the readings of time, load and settlement of pile head were taken and recorded for every increment and decrement at 0, 15, 30 and 60 minutes. Rate of loading and rate of unloading remains same.

5.4 Abandonment of load test

The test is discontinued if any of the following occurs:

- Pre-loading before the commencement of the test.
- Improper setting of datum.
- Faulty of pile cap or instability of the Kentledge.
- Faulty jack or gauge.
- Pile head crack or broken.
- Initial readings are incorrect.

5.5 Failure of test pile

If any of the following conditions is detected after the preliminary tests have been completed as stipulated above, the tested piles are judged to have failed or attained the ultimate load capacity.

- Pile material is broken.
- A settlement equal to 15% of the test pile diameter is recorded.
- The rate of settlement continues undiminished without further increment of load.



Table 3 Recorded Data of Static Pile Load Test

Elapsed Time	Read Time(min.)	Load (Tonnes)	Dial gauge Readings(mm)				Average Settlement (mm)	Rate of Settlement(mm/hr)	Remarks
			A	B	C	D			
8:00 AM	1	24.45	0.18	0.17	0.16	0.17	0.17		
	15		0.19	0.18	0.18	0.19	0.19		
	30		0.20	0.19	0.19	0.21	0.20		
	60		0.22	0.21	0.20	0.23	0.22	0.05	
9:00 AM	1	53.80	0.65	0.61	0.69	0.64	0.65		
	15		0.70	0.66	0.74	0.69	0.70		
	30		0.73	0.68	0.77	0.72	0.73		
	60		0.76	0.71	0.80	0.75	0.76	0.11	
10:00 AM	1	78.34	1.40	1.33	1.31	1.28	1.33		
	15		1.45	1.38	1.36	1.34	1.38		
	30		1.48	1.41	1.39	1.37	1.41		
	60		1.50	1.43	1.41	1.39	1.43	0.10	
11:00 AM	1	107.70	2.21	2.11	2.02	1.98	2.08		
	15		2.26	2.16	2.08	2.04	2.14		
	30		2.29	2.19	2.12	2.07	2.17		
	60		2.30	2.21	2.15	2.09	2.19	0.11	
12:00 PM	1	132.24	3.85	3.79	3.75	3.56	3.74		
	15		3.90	3.84	3.81	3.61	3.79		
	30		3.93	3.86	3.86	3.66	3.83		
	60		3.95	3.88	3.88	3.67	3.85	0.11	
1:00 PM	1	161.64	5.70	5.58	5.64	5.42	5.59		
	15		5.75	5.64	5.71	5.47	5.64		
	30		5.78	5.64	5.75	5.51	5.67		
	60		5.80	5.71	5.77	5.53	5.70	0.12	



2:00 PM	1	186.14	9.20	9.16	9.26	8.78	9.10	Settlement rate >0.25mm/hr
	15		9.72	9.59	9.87	9.26	9.61	
	30		10.13	9.98	10.39	9.69	10.05	1.05
	60		10.22	10.09	10.51	9.76	10.15	
	75		10.26	10.12	10.56	9.79	10.18	"
	90		10.29	10.14	10.60	9.81	10.21	0.16
3:30 PM	1	215.59	15.41	14.99	15.35	15.26	15.25	Settlement rate >0.25mm/hr
	15		16.32	15.88	16.26	16.06	16.13	
	30		16.93	16.55	16.87	16.60	16.74	1.98
	60		17.46	16.98	17.40	17.07	17.23	
	120		17.89	17.31	17.81	17.43	17.61	"
	180		18.24	17.52	18.13	17.68	17.89	"
	240		18.39	17.61	18.27	17.79	18.02	0.12
	300		18.48	17.64	18.35	17.83	18.08	0.06
8:30 PM	1	186.14	17.53	16.47	16.98	16.66	16.91	Settlement rate >0.25mm/hr
	60		17.48	16.44	16.95	16.62	16.87	
9:30 PM	1	161.64	16.91	16.07	16.51	16.19	16.42	-0.04
	60		16.84	16.05	16.46	16.15	16.38	-0.05
10:30 PM	1	132.24	16.18	15.56	15.82	15.63	15.80	Settlement rate >0.25mm/hr
	60		16.14	15.53	15.79	15.60	15.77	
11:30 PM	1	107.70	15.28	14.79	14.95	14.83	14.96	-0.03
	60		15.23	14.77	14.92	14.81	14.93	-0.05
12:30 AM	1	78.34	14.09	13.57	13.89	13.73	13.82	Settlement rate >0.25mm/hr
	60		14.02	13.55	13.84	13.68	13.77	
1:30 AM	1	53.80	12.67	12.34	12.51	12.47	12.50	-0.05
	60		12.59	12.31	12.45	12.43	12.45	-0.05
2:30 AM	1	24.45	10.96	10.57	10.79	10.68	10.75	Settlement rate >0.25mm/hr
	60		10.91	10.54	10.75	10.64	10.71	

7



8. Conclusions and Discussions

As per ASTM D 1143/D 1143M-07

The test load at which rapid, continuing, progressive movement occurs, or at which axial movement exceeds 15% of the pile diameter or width, is termed as failure load.

From the load settlement curve, the total settlement is found to be **18.08 mm**, which is within the permissible limit (i.e. 15% of pile diameter)

As per IS 2911 (part 4)

The safe load on a single pile shall be the least of the following (According to IS 2911 (part 4)):

For piles more than 600 mm diameter:

- Two-thirds of the final load at which the total displacement attains a value of 18 mm or maximum of 2 percent pile diameter whichever is less unless otherwise required in a given case on the basis of nature and type of structure in which case, the safe load should be corresponding to the stated total displacement permissible
- 50 percent of the final load at which the total displacement equal to 10 percent of the pile diameter in case of uniform diameter piles and 7.5 percent of bulb diameter in case of under-reamed piles.

From the load settlement curve, the total settlement is found to be **18.08 mm**, which is within the permissible limit. But as noted from the static load test of other bridge sites of the same project, the settlement of the piles were below 6mm. This pile has much higher settlement as compared to those piles. Besides, if we see at the rate of settlement data, it is observed that at 186.14 KN and 215.59 KN load, the rate of settlement is much higher (greater than 0.25mm/hr), which is questionable.

From the PIT test report, the pile do not have any integrity defect. According to the geotechnical report, the Soil Investigation shows, the soil condition around this test pile mostly are poorly graded sand with silt. The reason for higher settlement of the pile may be due to the presence of some loose pocket of sandy soil along the shaft or toe of the pile that were not detected during drilling. This may result in the actual friction are less than reported in geological reports.



1. GENERAL

1.1 Introduction

Integrity refers to the change in physical dimension, continuity of a pile, consistency of pile material. Pile integrity test is non-destructive test for evaluation of integrity in concrete piles. This procedure explains in detail the method statement conducting pile integrity test of cast in-situ pile of diameter 1000mm Mahuli Bridge.

1.2 Test Purpose

The purpose of pile integrity test is

- To determine the length of pile
- To evaluate the integrity of pile
- To check the consistency of pile material

1.3 Related Specification

The test shall generally be those recommended in ASTM C1740 Standard Test Method for Low Strain Impact Integrity Testing of Deep Foundations.

2. DETAILS OF TEST PILE

The location is decided by the Designer, Consultant or Employer. The details of test piles are shown in the following table:

Table 1 Pile Details

Location	Type	Code of Pile in Drawing	Pile Diameter mm	Pile length m	Date of Casting	Date of Testing
Pier	Cast in-situ	P6-PP3 Working Pile	1000	20	16 Dec 2021	17 Jan 2022

Additional Information

- The Test pile has 1.3m diameter up to a depth of 2.7m from the top followed by 1.0m diameter.
- The total estimated length of the pile during the test is 22.77m
- Required pile diameter = 1.0m
- RL of cutoff level of pile = 114.562m
- RL of Test level of pile = 117.26m

3. TEST METHOD

Pile Integrity Test can be applied to any concrete pile. The test is performed with a hand held hammer, an accelerometer or geophone and data acquisition and interpretation electronic instrument. Hammer is used to induce impact of low strain. An accelerometer or geophone measures the response of hammer impact. Data acquisition and interpretation electronic instrument display results.



1



Pooja Singh

Numerical Analysis of Laterally Loaded Pile in Sandy Soil

 Tribhuvan University

Document Details

Submission ID

trn:oid::3117:585893015

Submission Date

May 4, 2026, 8:32 PM GMT+5:45

Download Date

May 4, 2026, 11:24 PM GMT+5:45

File Name

Final_079msgte013_Final for plag.pdf

File Size

5.0 MB

94 Pages

17,586 Words

92,701 Characters

16% Overall Similarity

The combined total of all matches, including overlapping sources, for each database.

Filtered from the Report

- ▶ Bibliography
- ▶ Quoted Text
- ▶ Cited Text
- ▶ Small Matches (less than 8 words)

Custom Section Exclusions

{titlesCount} Section Titles, {keywordsCount} Keywords

Section title	No. of Section Starters	Section Starters
"Acknowledgements"	4	Acknowledgements Acknowledgement Acknowledgment Acknowledgments

Match Groups

- 🔴 **221 Not Cited or Quoted 16%**
 Matches with neither in-text citation nor quotation marks
- 🟠 **0 Missing Quotations 0%**
 Matches that are still very similar to source material
- 🟡 **0 Missing Citation 0%**
 Matches that have quotation marks, but no in-text citation
- 🟢 **0 Cited and Quoted 0%**
 Matches with in-text citation present, but no quotation marks

Top Sources

- 15% Internet sources
- 10% Publications
- 0% Submitted works (Student Papers)

Integrity Flags

0 Integrity Flags for Review

No suspicious text manipulations found.

Our system's algorithms look deeply at a document for any inconsistencies that would set it apart from a normal submission. If we notice something strange, we flag it for you to review.

A flag is not necessarily an indicator of a problem. However, we'd recommend you focus your attention there for further review.